FREIGHT MOBILITY RESEARCH INSTITUTE
College of Engineering & Computer Science
Florida Atlantic University

Project ID: Y2R6-18

MODELING THE IMPACTS OF WEATHER AND DEMAND UNCERTAINTIES ON UAVS FLEETS AND EMISSIONS

Report

by

Miguel Figliozzi, Ph.D.
Portland State University
Email: figliozzi@pdx.edu

for

Freight Mobility Research Institute (FMRI)
777 Glades Rd.
Florida Atlantic University
Boca Raton, FL 33431

October, 2020

ACKNOWLEDGEMENTS

This project was funded by the Freight Mobility Research Institute (FMRI), one of the twenty TIER University Transportation Centers that were selected in this nationwide competition, by the Office of the Assistant Secretary for Research and Technology (OST-R), U.S. Department of Transportation (US DOT).

DISCLAIMER

TABLE OF CONTENTS

LIST OF TABLES

LIST OF FIGURES

EXECUTIVE SUMMARY

Growing e-commerce volumes and consumer expectations of free and faster shipping are pushing the adoption of new delivery vehicles. New driverless air and ground vehicles are being launched and tested to deliver products or services by traditional package delivery companies or to support innovative ideas in retail, groceries, and healthcare.

For the delivery of time-sensitive supplies, drones may provide the means to bypass many obstacles experienced by ground transportation vehicles. However, drones are subject to their own set of constraints, like weather conditions and limited range, that limit the likelihood of successful deliveries. Drones are increasingly being utilized to deliver medical supplies, and the COVID-19 pandemic has accelerated this trend. Drones arrive quickly by taking more direct paths and avoiding ground-based obstructions. However, drones are not completely reliable and may also experience failures and delays. For consumer products, delivery delays are an inconvenience, but for some time-sensitive deliveries like medical supplies delays are likely to cause severe health impacts or even fatalities.

The number of drones needed when there is demand uncertainty is highly dependent on charge times, use of battery swapping, and population in the service area. Additional consideration should also be given to potential mechanical failures and maintenance schedules. It is important to note that failures due to extreme weather conditions cannot be addressed by simply having more available drones. Extreme weather conditions, which will result in a failed delivery for one drone, will result in a failed delivery for any other drone because drones cannot operate under extreme weather conditions. Wind is a key constraint for drone deliveries. Successful drone deliveries are highly influenced by wind speeds, wind direction, and precipitation rates; however, the ambient temperature may mostly be ignored for short delivery distances.

Furthermore, there is an access and equity question associated with a drone’s ability to deliver to some areas. For example, airports are often restricted flight zones that allow for no drone operations. Such areas are also areas with higher proportions of lower-income communities. Future research could examine where a delivery system could be employed and what ground delivery systems are required locally to adjust for access differences.

Another important aspect is the sustainability of drone deliveries. In terms of energy and emissions efficiency there is no vehicle type that dominates across the board. Drones are more efficient in time constrained and low-density delivery scenarios. Road autonomous delivery robots (RADRs) are more efficient than E-vans when delivering to relatively low number of customers. New air and ground autonomous vehicle types may reduce carbon emissions significantly but they may not necessarily reduce on-road travel. For some autonomous vehicles the reduction of on-road travel is also accompanied by additional travel on sidewalks (SADRs) or air travel (drones).

In summary, drones or Unmanned Aerial Vehicles (UAVs) can significantly improve the reliability of time-sensitive deliveries in urban and rural areas as well as reducing carbon emissions. Policy makers and regulators should seriously consider their benefits as well as potential safety risks related to malfunction or mid-air collisions.

1.0 INTRODUCTION

In recent years there has been a lot of exciting new developments and innovative applications of drone or Unmanned Aerial Vehicles (UAVs) in freight transportation and logistics. UAVs have the potential to reduce costs and delivery times and UAVs have been featured frequently in the media following announcements made by large corporations such as Amazon (Vincent and Gartenberg, 2019).

However, the sensitivity of UAVs to weather events and their potential impact on energy consumption and greenhouse gas (GHG) emissions are currently understudied. This research studies how weather affects drone operations and fleet size as well as the potential of drones to reduce carbon emissions in last mile deliveries. The focus of the modeling effort is on electric multicopters that weigh less than 20 kg given their potential for urban and rural deliveries as well as their relatively modest cost.

1.1 BACKGROUND

This section provides a brief background regarding drone-truck applications, fleet sizing, the impact of weather conditions, drone regulation, and drone carbon emissions.

1.1.1 Drone-Truck Routing and Optimization

The idea of utilizing both UAV and trucks (Murray and Chu, 2015) to improve overall delivery efficiency has also been analyzed by many authors focusing on the actual design of routes and logistics systems in the last five years. There has been an explosion in the number of papers related to drone optimization. Several reviews present an overview of modeling efforts. A survey of applications of drones in civil problems is presented by Otto et al. (2018). A more recent survey by Macrina et al. (2020) focuses mostly on routing problems with drones and the review by of Chung et al. (2020) on drone-truck combined operations.

1.1.2 Fleet sizing

Fleet sizing has also received scant attention in relation to drone routing. The work of Lee (2017) utilizes modularity and simulation in drone design to estimate fleet size optimize their operation. Rabta et al. (2018) studies last mile deliveries in humanitarian logistics using a MIP model where the objective minimizes the total travelling distance or cost taking into account drone payload and energy constraints and the installation of recharging stations. Chauhan et al. (2019) present a MIP formulation and heuristics to maximize drone fleet coverage also taking into account drone payload and energy constraints and providing facility location, allocating drones to facilities and drones to customers. This work is later extended to provide robust solutions when accounting for uncertainty in initial energy battery availability and energy consumption (Chauhan et al., 2020).

Torabbeigi et al. (2020) formulates a set covering problem and a MIP model, considering payload and battery consumption, to locate facilities and minimize the number of drones in a parcel delivery system.

Fleet sizing under demand uncertainty has been studied for specific time-sensitive applications. For example, Boutilier et al. (2017) takes into account spatial demand uncertainty and utilizes optimization and queuing to determine drone fleet size for the emergency delivery of automated external defibrillators. This work was extended by Glick et al. (2021) to include not only demand uncertainty but also the impact of weather conditions on drone fleet sizing.

1.1.3 Impact of Weather Conditions

Some researchers have analyzed the impact of weather conditions such as temperature on electric drone operations. For example, Kim et al. (2018) presents a robust optimization approach to find the optimal number of drones and flight paths taking into account that temperature affects battery performance. Similarly, Thibbotuwawa et al. studies drone flight path optimization under uncertain weather conditions (2020). Overall, at this time there is little research linking weather conditions and drone operations and fleet sizing.

1.1.4 Emissions

In terms of emissions, UAVs have many potential advantages. An analysis of lifecycle UAV and ground commercial vehicles CO2e emissions with different route and customer configurations showed that UAVs are more CO2e efficient, for small payloads, than conventional diesel vans in a per-distance basis (Figliozzi, 2017). However, UAV deliveries were not more CO2e efficient than tricycle or electric van delivery services if a few customers can be grouped in a route. Ground vehicles can be more efficient regarding emissions in dense urban areas where many customers can be grouped in a route; UAVs may be more efficient in remote rural areas (Figliozzi, 2017). However, the literature have not analyzed the relative emissions of drones against ground delivery robots.

1.1.5 Regulation

According to Stöcker et al. (2017) countries around the world have been steadily adopting regulations to minimize risk of UAV failures and collisions that can put in risk lives and property. These regulations are similar in many aspects to requirements that sidewalk autonomous delivery robots (SADR) and road autonomous delivery robots (RADR) must follow (Jennings and Figliozzi, 2019, 2020): registration and licensing, reducing speeds and or operating weight, and minimum levels of insurance and liability protection. In addition, for UAVs restrictions apply to airspace use such as maximum flight altitude and restrictions near critical infrastructure such as airports.

In the US, the Federal Aviation Administration (FAA) issued restrictions on the non-recreational use of unmanned aerial vehicles which effectively prohibited freight delivery using drones in the USA (FAA, 2016). Restrictions prevent any business from currently utilizing drones in a freight delivery service and require that drones must be flown using VLOS (visual line of sight) at all times which would greatly reduce the size of the service area, especially in forested hilly terrains or dense areas with skyscrapers, and reduce the economic benefit of not having a human pilot in the UAV. According to 2016 FAA rules, drones must not be flown over populated areas, less than 400' from any structure, when visibility is a less than three miles, and reduced daytime visibility. These restrictions allow freight to be delivered in rural environments over short distances and on very clear days. The 25 kg (55 lb) weight limit, which includes payload, does affect some of the drones currently found in the USA marketplace.

1.2 GOALS

UAVs or drones have the potential have many advantages and can disrupt last mile deliveries and supply chains. UAVs are not constrained by road infrastructure and/or congested roadways. UAVs can increase significantly last mile freight mobility for packages and small payloads. UAVs are likely to have a nationwide impact, in both urban and rural areas. However, UAVs are severely constrained by its limited range and by weather conditions. The goals of this research are to: (a) model and study the impacts of weather conditions such as wind, temperature, and rain on drone operations, (b) analyze fleet sizing given demand uncertainty for critical deliveries, and (c) compare drone last mile emissions against traditional and innovative ground vehicles such as ground delivery robots.

This report is organized as follows: after this introduction Section 2 presents a review of e-commerce and package delivery trends. Section 3 studies fleet sizing for time-sensitive and stochastic deliveries. Section 4 discusses weather modeling and Section 5 studies the impacts of weather conditions on drone range. Section 6 presents the modeling framework to analyze energy and emissions. Sections 7 and 8 presents and discusses energy, distance, and CO2 emissions results comparing drones to alternative delivery vehicles. Section 9 ends with conclusions.

2.0 E-COMMERCE TRENDS AND PACKAGES

According to the United States Quarterly E-Commerce Report, e-commerce sales in the United States (US) have increased at double digit rates for the past two decades (USDC, 2020). During this time, e-commerce has outpaced brick-and-mortar retail growth, both in the United States and globally. Some online stores promote an in-store pickup service, but the large majority of online customers have products delivered to their residence, their work, or another location of their choice. Though some authors distinguish between retailers (sales revenue is primarily generated offline) and e-tailers (sales revenue is primarily generated online), this section will use the term retailer to refer broadly to sellers, and the specifiers "in-store," "brick-and-mortar," "online," and "e-commerce" will be used as necessary.

2.1 E-COMMERCE INTERNATIONAL TRENDS

Global statistics show a general increase in e-commerce sales, but the rate of adoption varies greatly by country. E-commerce remains a minority fraction of total retail volume, but further growth is expected before market saturation is achieved. For overall e-commerce volume, China's leads globally with over $1T of e-commerce sales projected for 2020, and for 2017–2019, its average year-over-year (YoY) increase was +24.5%. During the same time, e-commerce in the United States grew steadily with an average YoY increase of +11.5%. The United Kingdom was clearly an early e-commerce adopter, but by 2018, the e-commerce market of Japan was larger. India had the steepest shift to e-commerce with average year-over-year sales increases of +35.0% YoY. In the selected countries, no market showed a decrease in online shopping. Figure 1 shows recent trajectory of e-commerce, including 2020 forecasted volume, which was adjusted in June 2020 due to COVID-19 pandemic (Statista, 2020). Figure 1 includes only the following products: fashion, electronics, toys/hobby, furniture, food & personal care.

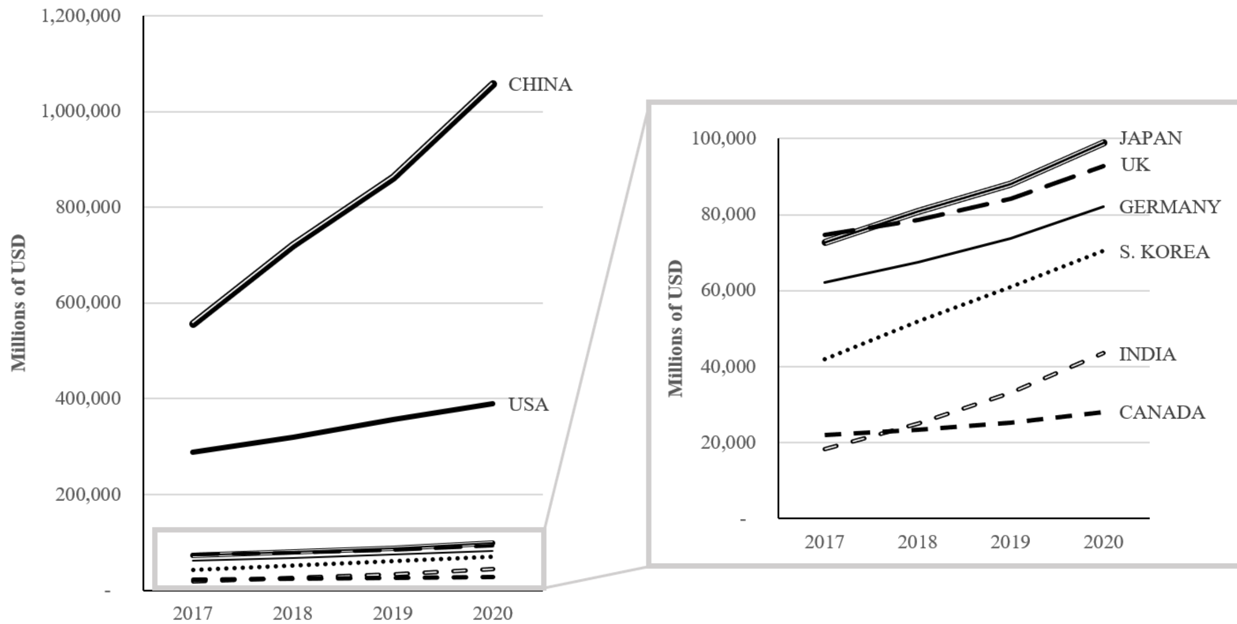

Figure 1: International Comparison E-commerce sales 2017–2020

There are no signs of e-commerce markets contracting in the near future. Sales volumes projections (Figure 2) through 2024 for selected countries expect significant e-commerce increases, with China forecast to remain the top e-commerce consuming nation (Statista, 2020). Figure 2 includes only the following products: fashion, electronics, toys/hobby, furniture, food & personal care. India is expected to grow fastest during the same time period, but the total dollar volume is projected to be relatively low compared to China and the USA. Even for countries–such as the United States–where 2024 projections of e-commerce remain a minority portion of total retail volume, the anticipated increase of home deliveries represents a massive uptick in freight trip activity.

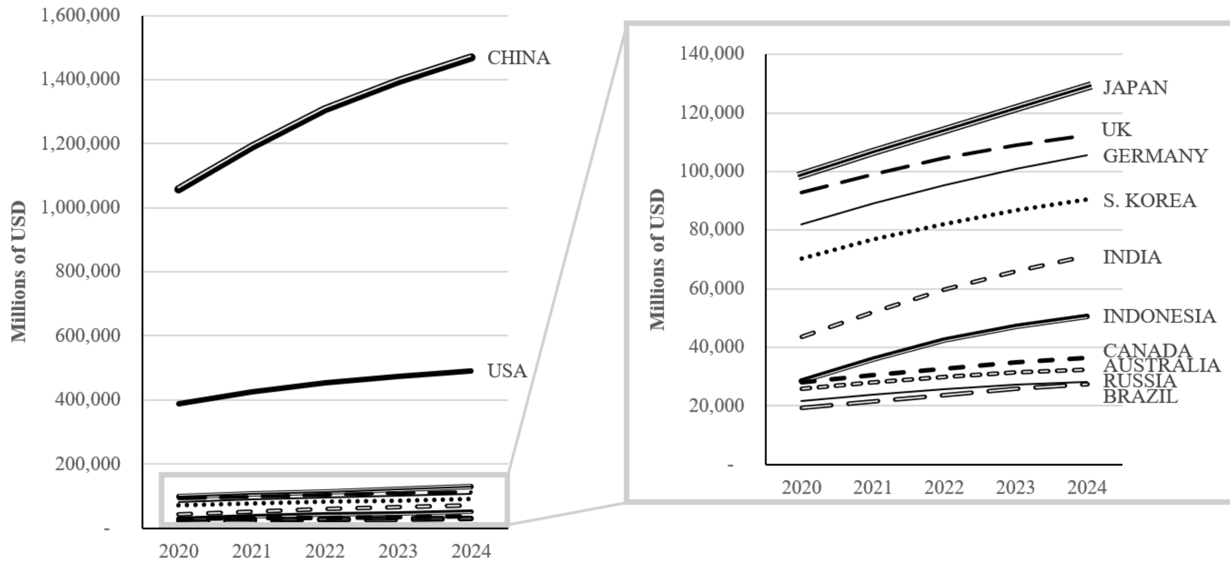

Figure 2: E-commerce forecasted sales 2020–2024.

2.2 US PACKAGE DELIVERY TRENDS, 2015–2019

Between 2015–2019, US major couriers FedEx, UPS, and United States Postal Service (USPS) all exhibited growth in the number of packages shipped (FedEx Corporation, 2018; 2019) (UPS of America Inc., 2018; 2020) (USPS Corporate Communications, 2020). By the end of fiscal year 2019, 1.52 billion packages were shipped domestically, a +27.5% increase from 2015. By company, FedEx package volumes grew +23.5% and UPS's grew +19.3% over the same period. USPS package volume–which includes Priority Mail, Priority Mail Express, First-Class Package, Parcel Return Service, and Parcel Select–increased by +37.8%, from 4.5B to 6.2B pieces. Conversely, USPS's volume of first-class (flat) mail declined from 62.6B to 54.9B pieces. This signals the shift in mail streams from postage stamps to shipping labels, as can be attributed to e-commerce demand.

FedEx Ground grew dramatically (+29.5%) but their air cargo service, FedEx Express, saw relatively modest growth (+8.1%). Unlike FedEx Express, UPS's Next Day Air dramatically increased by +43.0%. UPS Deferred (a service slower than Next Day Air but faster than Ground) and UPS Ground services saw moderate increases but were relatively less than the growth of FedEx Ground. The increase in package circulation correlates with the increase in e-commerce sales, but it should be noted that the figures in

Table 1 represent total packages shipped, whether associated with e-commerce or not.

Table 1: Number of packages annually*, US domestic (in millions).

Courier	2015	2016	2017	2018	2019	Vol. change 2015-2019	% Change 2015-2019
FedEx Express	979	990	995	996	1,059	80	8.1%
FedEx Ground	2,523	2,747	2,882	3,043	3,267	745	29.5%
UPS Next Day Air	334	352	371	390	478	144	43.0%
UPS Deferred	334	345	356	362	410	77	23.0%
UPS Ground	3,294	3,446	3,571	3,668	3,840	545	16.56%
USPS	4,500	5,200	5,700	6,200	6,200	1,700	37.80%
TOTAL	11,964	13,080	13,875	14,659	15,254	3,290	27.5%

**Fiscal year ends Dec 31st for UPS and USPS; fiscal year ends Mar 31st for FedEx.*
(FedEx, 2018; 2019) (UPS, 2018; 2020) (USPS, 2020)

With all three major US couriers showing strong growth in recent years, the overall momentum of package circulation is apparent. It is no longer unusual to see parcels on residential doorsteps, with many consumers receiving shipments almost daily. The logistics of transporting the package to final delivery must be reliable and efficient. As more producers and retailers deliver directly to the end user, it is critical to understand timeframes, operations, and product destinations, as they will shape future delivery modes and receiving technologies. FedEx expects US parcel delivery to increase to 100 million packages per day by 2026 (Sutherland, 2019), so transitioning towards the impending scale of associated freight trips will have implications for both retail stakeholders and transportation practitioners.

2.3 US E-COMMERCE CONSUMER DEMOGRAPHICS

Who is purchasing e-commerce goods? In the United States, urban dwellers are more likely to purchase online for home delivery than their rural counterparts (FHWA, 2018). According to the 2017 National Household Travel Survey, about 56% of urbanites purchased online at least monthly, compared to 51% of rural residents. (This may be attributed to the relatively limited availability of broadband networks in rural areas.) Online platforms have successfully reached holiday consumers; in 2017, people living in urban, suburban, and rural settings all widely used e-commerce for seasonal purchases (Statista Survey, 2017b). No categories of US shoppers utilized online shopping for 100% of holiday shopping, but urban dwellers were more likely to shop online than rural residents, with suburban households purchasing online most frequently. Though not everyone embraces e-commerce, in 2017, about 60% of internet users purchased online at least monthly, with 29% of this same group purchasing at least once per week (Walker Sands, 2017).

Recent surveys find that 43% of American consumers cite convenience as their strongest motivator for shopping online, and pricing is a distant second at 19% (eMarketer, 2018b). Across all age categories, e-commerce has been widely adopted, and Amazon was the most popular online marketplace (Table 2). However different age groups vary in their means of internet access and types of product purchased (eMarketer, 2018a). The only age category for which over half of respondents did not use Amazon was the 60+group. Young adults were most likely to make purchases via smartphone; about 60% of shoppers aged 18-29 report smartphone shopping.

Table 2: US online shopping activity by internet users, by age.

	Percentage of Age Group					
Shopping Activity	**18-29**	**30-39**	**40-49**	**50-59**	**60+**	**Total**
Purchased a product on Amazon.com or Amazon app using Amazon Prime	59.6	65.0	57.4	51.1	48.1	54.4
Researched a product digitally before purchasing in-store	55.8	54.0	51.1	42.4	39.2	46.1
Purchased via an online marketplace (e.g., Amazon independent sellers, Etsy, Wish)	50.0	46.5	41.6	45.9	41.0	44.0
Purchased via a smartphone	60.6	58.0	40.5	27.9	19.0	35.5
Purchased a product through a retailer's rewards program (e.g. Amazon Prime, Sephora, Ulta)	47.1	39.0	35.3	24.5	25.2	31.3
Purchased digitally and picked up in-store	26.9	36.5	30.0	27.9	23.6	28.2
Looked at a product in-store before purchasing it digitally	36.5	31.0	28.4	23.1	17.4	24.7
Purchased a travel product/service (e.g. airline tickets, hotel, rental car)	26.9	25.5	20.0	20.1	18.4	21.1
Heard about a product via social media, then purchased it	31.7	28.0	21.6	19.7	11.4	19.8
Used a shared economy service (e.g. Airbnb, Lyft, Uber)	37.5	21.5	12.1	7	6.2	13.1
Purchased from a website based outside of the US	12.5	15.0	10.0	13.5	9.4	11.6
Received a subscription box (e.g. Blue Apron, Birchbox, ipsy, Stitch Fix)	12.5	15.0	11.6	7.9	3.6	8.8
Bought using voice-enabled speaker (e.g. via Alexa, Amazon Echo, Google Home)	1.0	4.5	4.2	3.5	2.9	3.3
None of these	3.8	4.0	4.7	5.7	10.9	6.9

(eMarketer, 2018a)

The relationship between age categories and online purchasing may be studied further, as different age categories often elect different housing types. This can affect the efficiency of urban deliveries as well as the types of goods ordered. For example, younger Americans are more likely to live in apartments or in group living arrangements, and some older Americans live in senior communities, which are often on the less densely developed edges of urbanized areas where land is less expensive.

2.4 SHIPPING COSTS AND CONSUMER PURCHASING DECISIONS

2.4.1 Consumer willingness-to-pay, or lack thereof

Shipping costs hold weighty influence in e-commerce consumers' purchasing decisions. According to a UPS study, shipping fees are a significant contributor to failed sales, with an estimated 41% percent of carts abandoned after shipping costs are presented (UPS, 2019). E-commerce businesses know they must meet consumer expectations, which puts significant pressure on the pricing process. Convenience is prioritized, but its value does not readily translate into an acceptance of the premiums required to the quickly transport goods to front doors.

A study about delivery of online purchases in London indicates that there is a "mismatch between what people are willing to pay for the delivery and the [true] cost of providing the delivery service" (Allen et al, 2018). A 2016 report by UK consultants OC&C estimated the last mile shipping costs the e-commerce retailer to be 5–23 times more expensive than the same sale in a store (cited in Allen et al, 2018). This is corroborated by other studies finding online channels to be less profitable than in-store channels whenever return rates are high or consumers are not willing to pay for delivery (Kumar and Ruan, 2006) (Zhang et al, 2017).

Even as "free" shipping has been promoted enough to be fairly normalized, the actual logistics of package shipments cost money–and shipping companies are not in business to lose money. Aircraft and delivery trucks represent major capital expenditures, and employee salaries and vehicle fuel are ongoing expenses. Further imbedded costs include real estate expenses for freight depots, delivery vehicle staging areas, warehousing in the urban periphery, as well as the extra transportation costs between warehouse districts and urban delivery destinations. For most consumers, these complex operations happen behind the scenes, and the out-of-sight nature of logistics undermines customers' ability to accurately recognize the value in home delivery. Table 3 further details consumer reactions to shipping costs.

Table 3: Influence of Shipping Costs in Online Shopping for US Shoppers in 2017.

I cancel my order if the shipping costs are too high	57%
High shipping costs make me think twice about whether I actually want a given product	54%
I tend to order more often from shops that offer free shipping	45%
I always make sure that I can return everything free of charge	15%
High shipping costs make me order rather more, so I feel like it is worth paying them	5%
Shipping costs have no influence on my purchase decision	2%

(Statista Survey, 2017a).

2.4.2 Retailer approaches to pricing shipping

Retailers are caught between demands for expedient shipments and consumer aversion to increased shipping costs. Depending on their commodity dimensions and target consumer, e-commerce retailers must choose a pricing strategy to cover shipping expenses. Some offer lower prices with higher shipping costs (partitioned prices) while other retailers offer higher prices on goods sold but free shipping while still others offer free shipping beyond a certain amount of spending (Frischmann, 2014). These strategies appeal to different types of online customers. Indications are that retailers offering "free" shipping actually charge more than online retailers with partitioned prices, as the price of "free shipping" is factored into the retail price of the goods sold online. Some on-demand delivery services such as Amazon Prime and Walmart Grocery offer free delivery as a privilege of their annual membership fee; this appeals to customers who can sink the cost to secure a prepaid cap on their shipping expenses (Keeling and Figliozzi, 2019).

2.4.3 Free shipping promotions

Free shipping is a conundrum for e-commerce. To promote free shipping, retailers must titrate the true shipping costs into product retail values. However, to support the perception of free shipping, online prices must be competitive with those of brick-and-mortar stores. For shoppers only interested in purchasing from e-commerce vendors, price transparency would be beneficial to consumers because retailers must compete on shipping costs (Shao, 2017). But the competition would be fierce as Shao also referenced a 2008 study indicating that 72% of online shoppers would abandon a virtual shopping cart if free shipping were available from another online retailer. With consumers having easy online access to vast amounts of pricing information, customers can easily shop around for the best price including free or reduced cost shipping. As such, Shao's models find that free shipping is the most broadly effective policy to increase sales.

Free shipping can increase consumer acquisition, but customer loyalty may prove fickle if consumers view free shipping as requisite for purchase. During the advent of e-commerce in the late 1990s and early 2000s, e-commerce offered free shipping to incentivize people to convert to online purchasing. As a result, consumers are now conditioned to expect free shipping. Many media articles penned by retail industry leaders bemoan this consumer expectation as financially unsustainable, as it positions retailers as loss leaders (Ungerleider, 2016). The CEO of Hudson's Bay Company estimates it costs three times more in supply chain costs to serve an online customer versus serving the same customer in an actual store. Bob Schwartz, best known for founding Nordstrom.com, contends that because Amazon has nearly-unrivaled advantages in investor backing, economy of scale, and supplementary revenue streams, it is unbridled from immediate profitability and can pressure other retailers to feed into their own free shipping crisis.

In addition to shipping costs, e-commerce direct delivery extends the retailer's customer service obligations to the product's end reception, including shipping factors beyond their control. When shipping is bundled into the retail price, e-commerce consumers are not disincentivized for incurring additional costs (Allen et al, 2018). Shoppers may even purchase additional goods to meet minimum free shipping thresholds–and later return items they do not need. Unless a restocking fee is part of the return policy, the retailer will lose profit through carrying costs, labor, and shipping costs. Even for e-commerce retailers that outsource the actual shipping of goods, the accumulation of shipping cost ultimately inflates the price of goods.

All articles surveyed about this subject indicate free shipping is an important aspect of e-commerce and choices consumers make. How this is assessed varies from study to study and may change over time. Shipping is a volatile aspect of the retail business and change should be expected.

2.4.4 Competitive lead times

The time that lapses between the placement of an order and the time of delivery, (e.g. the lead time) is a value determinant for customers. Overnight shipping is no longer the most premium service now that on-demand (e.g. lead time < 1 day) shipping options are expanding. Some online retailers stage products in warehouses near major population centers, so products available for on-demand delivery can reach their destination within a few hours. For shippers, the per-item shipping rates for Amazon's US domestic shipping varies between $4 (for delivery within 7 days) and $20+ (for 1-day shipping), depending on weight of the item (Amazon.com, Inc., 2018). Not only does a short lead time increase the cost of delivery, but the narrowness of the acceptable delivery window does as well (Gevaers et al, 2014). However, a report by United Parcel Service states that consumers generally opt for competitive cost over competitive speed (UPS, 2019).

For last mile logistics, costs, on-time reliability, and the ability to respond to last-minute changes are the top concerns of logistics providers, manufacturers, and retailers. As increasing numbers of delivery carriers navigate through road networks alongside many other roadside users, curb access will become a greater determinant of on-time delivery. Both retailers and shippers are stakeholders in last mile issues; efficiency losses in delivery will increase shipping costs and decrease competitiveness. Couriers and shipping companies will be investing in the development of delivery innovations that can mitigate or circumvent these challenges.

2.5 THE COST OF FAILED VISITS AND RETURNS

What happens when an item is returned? All retailer will experience customers that want to return an item after purchase. E-commerce poses special problems as products ordered online likely come from a central warehouse and a third party makes the actual delivery. Returns are an enormous cost for retailers; the United States National Retail Federation reports that 9.6% of online sales were returned in 2019, representing nearly $41B in volume (Appriss, 2020). Most e-commerce consumers return up to a quarter of all products they purchase online, and some consumers return items even more frequently (Statista Survey, 2017c).

The reverse logistics of returned items are tricky. Retailers with physical locations will often accept returns of items ordered online and shipped direct; this has earned the acronym BORIS: buy online, return in-store. In fact, many retailers seem to prefer BORIS because consumers may make impulse purchases while in the store. Unfortunately, BORIS has been exploited for illegitimate returns for unwarranted credit, a fraudulent activity that further erodes retailer profits (Table 4). However, about two-thirds of returns are handled the same way they arrived on the consumer's doorstep–via a third-party shipping company. This could mean a consumer boxed the item back up and mailed it from a post office, or a delivery company picks up the item to return it to the originating retailer.

Table 4: Summary of returns and return fraud in the US.

Retail category	USD, billions
Total retail industry sales	$3,810
E-commerce sales	$426.7
Online returns	$41.0
Online return, BORIS	$20.5
Online return fraud, BORIS	$1.6

Online returns to non-store locations	$17.1
Online return fraud to non-store locations	$0.4

(Appriss, 2020)

The cost and rate of returns from e-commerce is greater than the return burden of brick and mortar stores, especially for some product categories. In the UK, up to 20% of all clothing purchased online is returned (Table 5); this return rate is nearly double that of off-line clothing stores (Bernon et al, 2016). Many online customers purchase multiple sizes of the same clothing style, try the clothing on when it arrives and then ship the unwanted pieces back. This creates logistical challenges for retailers: stock becomes unbalanced, online purchases are returned to retail stores, and returned products may need to be shipped elsewhere in the same store's retail system. For time-sensitive retail categories, products lose value while in circulation. There have been cases where retail stores have negative sales volumes, from accepting a volume of online returns exceeding the volume in-store sales (Bernon et al, 2016).

Table 5: Percent of product returns in the United Kingdom by category

Type of Product	Average	Highest	Lowest
Retail Store			
Clothing	10.9	19	4.9
Electrical/Technical	8.7	13.3	5.9
Home	5.5	11	1.5
Online			
Clothing	20	38.2	8.1
Electrical/Technical	8.0	10.3	6.4
Home	8.5	12.7	5.0

(Bernon et al, 2016)

Department store retailer Nordstrom is opening return-oriented storefronts, including three Nordstrom Local stores in the Los Angeles area since 2017, with more return-locations planned to open in the near future (Meyersohn, 2019). These locations will focus on receiving online orders for customer pickup, facilitating returns, and on-site tailoring and alteration services, something that may reduce the number of returned items. If customers can return unwanted products to a brick and mortar store, the retailer is likely to save money; for example, if 40% of returns can be channeled through a store rather than being sent back using a delivery service, retail profit margins could increase by seven percent (Capgemini Research Institute, 2019).

Some online retailers have started opening brick and mortar locations, with the hope many customers will instead return products in a more traditional fashion instead of just shipping them back the same way they arrived, via a package delivery service (Dennis, 2018). Industry experts are concerned that for many e-retailers, the rate of returns for online purchases is higher than in-store purchases, and the expectations of full refunds are often more pronounced for online purchases compared with traditional retail.

Some companies preemptively provide bags for returns in case the customer isn't pleased with the delivered product. Such is true for Jack Threads, an online-only clothing company. For their return policy, a customer is charged if they don't return clothing within seven days of delivery (Ungerleider, 2016).The CEO of Jack Threads feels offering free shipping (including reverse shipping) is necessary to make the customer happy and free shipping likely converts a first time purchaser to a long term customer. The number of times a package handling company visits a customer’s home also needs to be considered, especially for returns and a replacement product. If a customer returns an item by shipping it back to the retailer, a minimum of three visits must be made if the customer orders a replacement for the unwanted item. First, the initial item is delivered, then the returned item is picked up and finally, the replacement item is delivered (Bernon et al, 2016). While customers sometimes bear the burden of return costs, the majority of return shipping costs are borne by the retailer.

3.0 MODELING TIME-SENSITIVE DELIVERIES

The previous sections highlighted the growth of e-commerce and parcel deliveries in the US and abroad. Drones are particularly useful in areas with difficult access (Chauhan et al., 2019), e.g. remote or mountainous regions, or where traffic congestion increases delivery costs and reliability (Figliozzi, 2011). Reliability and speed delivery are key factors as mentioned in the previous sections, customers are sensitive to costs but at the same time companies and customers are pushing for increasingly more expensive shorter delivery times.

3.1 BACKGROUND

One of the best examples of time-sensitive deliveries are health related products and services. Due to the availability of data and without loss of generality, the following sections study the modeling of time-sensitive medical supplies. The delivery of medical supplies is an area that has sparked high interest because such supplies are often subject to strict temporal constraints. For example, drones have already been employed for the delivery of medical supplies in Rwanda, a country that experiences heavy rains that often lead to road impassibility (Ministry of Infrastructure, 2012). Hospital supply chains in Rwanda now utilize drones for the delivery of blood from central storage facilities (Chen, 2017) (Denby, 2019). While blood deliveries are time-sensitive, some medical supplies are subject to even more stringent time considerations. The COVID-19 and the consequent lockdown have temporality remove some regulatory barriers for the deployment of drones. Drones are now being tested in several states such as Florida, North Carolina, North Dakota and Virginia to deliver prescriptions, and there is a promising trial in Baltimore to deliver kidneys for transplants (Scalea, et al., 2018). Even though there is a wide range of drone applications in the health sector, this research and case study focuses on time-sensitive cardiac arrests.

Cardiac defibrillation (Brooks, et al., 2010) needs to be administered minutes after diagnosis to avoid patient death, but a majority (63%) of cardiac arrest cases occur outside of hospitals where defibrillators are not readily available. The survival rate for out-of-hospital cardiac arrest (OHCA) in 2016 was 12%, almost half that of the in-hospital rate (25%) (American Heart Association, 2018). Currently, automatic external defibrillators (AED) are 1.1 kg (2.4 lb), take just 1.77 L (108 in3) of space, and come with instructions to guide non-medical persons through the machine's use. This makes AEDs an ideal candidate for drone delivery. However, the seriousness of cardiac arrest puts tight constraints on adequate arrival times. Even in hospitals, defibrillation survival rates after 3 minutes are reduced from 39% to 22%, and each additional minute reduces the chance of survival by approximately 4% (Chan, et al., 2008). Currently, the average ground-based (ambulance) emergency response time in the United States is much longer than three minutes, with a mean of 7.0, 7.7, and 14.5 minutes for urban, suburban, and rural areas, respectively (Mell, et al., 2017). As drones are not subject to the typical ground road infrastructure restrictions, they may have a higher probability of timely response.

Pilots for medical supply deliveries using drones have begun in the United States (Glover & Colton, 2019), and recent research into drone deliveries of AEDs has attempted to quantify delivery times, estimate mortality rates, and optimize delivery networks through theoretical models (Claesson, et al., 2017) (Pulver & Wei, 2018) (Boutilier, et al., 2017). These studies have provided useful tools for AED delivery but have ignored key factors, such as weather. Such exclusions and the lack of real-world data means the viability of drone deliveries for time-sensitive supplies remains an open question.

This research focuses on drone deliveries of AEDs for OHCA and fills a gap in recent research by using real-world data to model and assess the impact of weather on drone delivery reliability and to quantify the impact of fleet size and population on failure rates. Determining the number of drones required to service an area is a difficult challenge as the rate of cardiac events for an area is dependent on population size and time of day (Brooks, et al., 2010). This research: first, models demand and estimates failure rates as a function of drone fleet size and population for two types of drone operations: battery recharging and battery swapping; second, model temperature, precipitation, and wind using historical data from Portland, OR; and third, quantifies the impact of temperature, precipitation, and wind on the range and drone delivery failure. Conclusions, based on results, are discussed with recommendations for future studies.

3.2 CASE STUDY

The American Heart Association (AHA) provides a population mean (μ_N) and confidence intervals (CI) for the number of OHCA events in a year (American Heart Association, 2018). From the CI, a population variance (σ_N^2) may be calculated. μ_N and σ_N^2 are for the US population as a whole (N), not for a selected sample of n people. For a sample population over a year, the mean and standard deviation for the number of OHCA may be calculated as:

$$\mu_N = 356{,}461 \qquad \sigma_N = 3{,}067$$

$$\mu_n = \left(\frac{n}{N}\right)\mu_N \qquad \sigma_n = \sqrt{\left(\frac{n}{N}\right)\sigma_N^2}$$

Modeling the number of occurrences in a given time interval is a common application of the Poisson distribution with parameter λ_n. To capture the variation of λ_n for a given population, λ_n is also simulated using a Gamma distribution with shape and rate parameters α and β, respectively. In Bayesian statistics, the Gamma distribution is the conjugate prior for Poisson, and equations for the mean and variance may be defined as follows (Casella & Berger, 2002).

$$E[\lambda_n] = \mu_n = \frac{\alpha}{\beta} \qquad Var[\lambda_n] = \sigma_n^2 = \frac{\alpha}{\beta^2}$$

Solving for α and β, the parameters of the gamma distribution for λ_n are:

$$\alpha = \frac{\mu_n^2}{\sigma_n^2} = \frac{\left(\left(\frac{n}{N}\right)\mu_N\right)^2}{\left(\frac{n}{N}\right)\sigma_N^2} = \left(\frac{n}{N}\right)\frac{\mu_N^2}{\sigma_N^2} \qquad \beta = \frac{\mu_n}{\sigma_n^2} = \frac{\left(\frac{n}{N}\right)\mu_N}{\left(\frac{n}{N}\right)\sigma_N^2} = \frac{\mu_N}{\sigma_N^2}$$

For any population, n, the number of cardiac events in a year may be simulated using:

$$\lambda_n \sim Gamma\left(\alpha = \left(\frac{n}{N}\right)\frac{\mu_N^2}{\sigma_N^2}, \beta = \frac{\mu_N}{\sigma_N^2}\right)$$

Given this formulation, random OHCA events are simulated using a Poisson distribution with rate parameter, λ_n, defined by AHA data. The above provides estimates for a full year. However, the number of OHCA is also temporally dependent.

There is no statistically significant variation across months or seasons, but day-of-week and time-of-day do have significant variation. Incidence rate ratios (IRR) with 95% confidence intervals are used for simulation, where the highest increases are seen on Mondays [1.18, 1.38] and during the 8:00 AM to 9:00 AM hour [1.96, 2.59] (Nordenskjöld, et al., 2019). Combined, Monday mornings have an average rate increase of 2.91 over the yearly average OHCA rate. Normal distributions are assumed for each IRR, based on the Central Limit Theorem of probability (Casella & Berger, 2002), and the time between consecutive OHCA events may be simulated utilizing a Poisson process of rate λ_n.

Figure 3 shows the asymmetry of the distribution around the mean for the time between events as a function of population size: for US average demand rate (left) and rate on Monday between 8:00 AM and 9:00 AM (right)

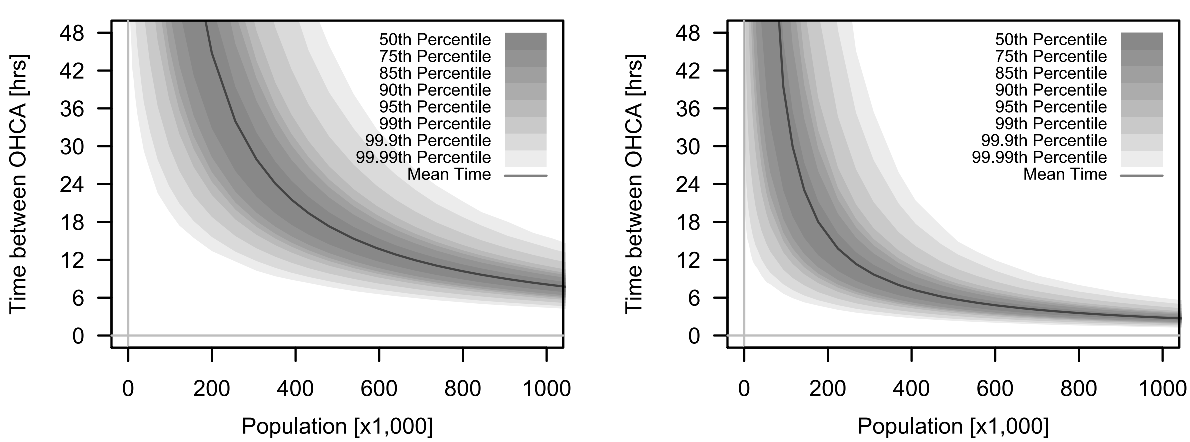

Figure 3 Time between consecutive OHCA events versus population

3.3 FLEET SIZE, DRONE REPOSITIONING, AND BATTERY SWAPPING TIMES

The number of required drones is based on the shortest time between events, given the nearly three-times increase over the average rates for Monday mornings, but also on the time it takes to serve a patient and reposition a drone. The calculated number of drones is, therefore the minimum required during peak demand and above the minimum for all other days-of-the-week and times-of-day. Two options are considered: in-drone battery recharging and battery swapping. For this study, we assume that a high-performance multi-copter MD4-3000 drone is utilized. Drone specifications are given in Table 6 (Figliozzi, 2017).

The optimal range is assumed to be 50 km (31 mi), which assumes ideal weather conditions and a cruise speed of 20 m/s (44.7 mph). With a 1.1 kg (2.4 lb) payload, the flight time will be approximately 42 minutes. The battery capacity of drones used in this study has a 21,000mAh (microdrones, 2019). The LiPo battery has a recommended recharge rate of 2A at greater than 90% charge efficiency (Alibaba, 2019). Therefore, the charge time following a complete drain of the battery for one of these drones is between 10 hours 30 minutes and 11 hours 40 minutes. However, batteries will not experience a full drain each time they are used, and there will be additional variability in the charge times based on distance traveled.

Table 6 MD4-3000 drone characteristics

3.4 SPECIFICATION	3.5 MD4-3000
Take off / Gross weight m	11.1 kg (24.5 lb)
Tare / Curb Weight m_t	10.0 kg (22.1 lb)
Payload m_l	1.1 kg (2.4 lb)
Empty weight factor c_m	0.90
Battery/Fuel Storage Capacity*	777 wh
Loaded Flight Time ($m_l = 1.1$ kg)	42 minutes
Range ($m_l = 1.1$ kg)	50 km (31 mi)

Given the random distribution of OHCA events and the combination of service and charge time of batteries, M/M/c queuing theory may be employed to determine the number of needed drones. For service times, it is assumed that a drone must stay with a patient until paramedics arrive (an average of 8 minutes) (Mell, et al., 2017), stabilize the patient (averaging 2 minutes), have the automatic defibrillator repackaged for the return trip (averaging 5 minutes), and return to base (averaging 5 minutes of flight and landing time). In addition to these 20 minutes of service times, drones are additionally unavailable to service new patients while their batteries are recharged (case 1) or swapped for a fully charged battery (case 2).

In case 1, given an average of 10 minutes of active flight time to and from a patient and the available flight time of 42 minutes, the average recharge time will be about 2 hours 40 minutes. Adding the 20 minutes of service time, the average usage time is 3 hours, which corresponds to an average of 8 possible services per day. Using an M/M/c queueing model, failure was defined as the probability that there will be one or more people in the queue (i.e., a person is waiting to be served due to drone unavailability). The rate of OHCA (λ_n) used is the worst-case scenario (i.e., 8:00 AM – 9:00 AM on Mondays). Figure 4 shows failure probability (plotted logarithmically) for case 1 (battery recharging), as a function of population and the number of available drones. In case 2 (battery swapping), after 20 minutes of average service time, each drone is assumed unavailable for an additional 10 minutes (30 minutes total) to allow for the battery to be swapped with a fully charged battery. In both cases the results are for demand rate on Mondays between 8:00 AM – 9:00 AM.

Figure 5 gives failure probabilities for case 2 given M/M/c queuing theory using the Monday morning rate. By swapping batteries, the number of possible services per day increases by a factor of 6, from 8 (in case 1, battery recharging) to 48 (in case 2, battery swapping) given the demand rate on Mondays between 8:00 AM – 9:00 AM.

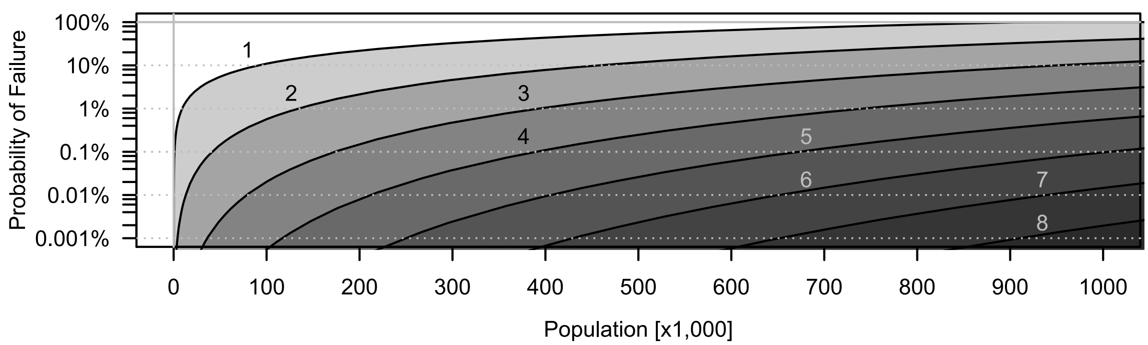

Figure 4 Battery Recharging failure probability vs. population and number of drones

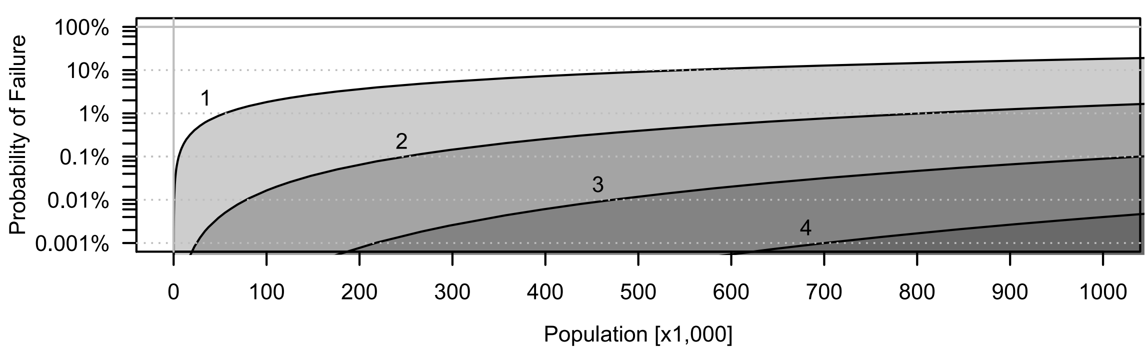

Figure 5 Battery Swapping failure probability vs population and number of drones

For 100,000 people on Monday mornings, a single drone would fail to provide service 10.9% of the time in case 1 versus just 1.8% of the time in case 2. Picking an acceptable failure rate for vital medical supplies of <0.1%, three drones are required in case 1, and two drones are required in case 2. For 300,000 people and a <0.01% failure rate, five and three drones are case 1 and 2, respectively. This difference corresponds to notable cost savings; each drone can cost between \$50,000 – \$100,000 (Aniwaa, 2019), but batteries cost between \$300 – \$600 (Alibaba, 2019). For 300,000 people and a failure rate of <0.01%, consider a theoretical requirement of one extra drone in both cases; and one or ten spare batteries per drone in cases 1 and 2, respectively. Equipment costs are 30% less in case 2 than in case 1. Lastly, other extreme conditions, such as those caused by wildfires, are also a potential issue, but outside the scope of the paper given the lack of detailed long-term wildfire data, the unique complexity of this topic, and the unusual set of operating constraints. A further potential issue is maintenance time and mechanical reliability of drones, but this topic is also outside of the scope of the paper due to the lack of drone reliability data.

4.0 WEATHER MODELING

The drone range and speed is affected by weather conditions, in particular wind intensity and direction, temperature, and rain or snow. This section presents a statistical approach to process whether data for drone delivery models.

4.1 MODELING TEMPERATURE DATA AND DISTRIBUTIONS

Historical temperature data for a region typically gives a mean, high, and low temperature for each daily record. Figure 6 shows a histogram and normal approximation of January and July daily high temperatures from historical tables from Portland, OR. Given the shape of the temperature histograms, each month's high and low temperatures are assumed to follow a normal distribution. Therefore, historical data provides the ability to calculate means for high and low temperatures and their respective standard deviations for simulation. However, on a given day, high and low temperatures are highly correlated, and this must be considered for simulations.

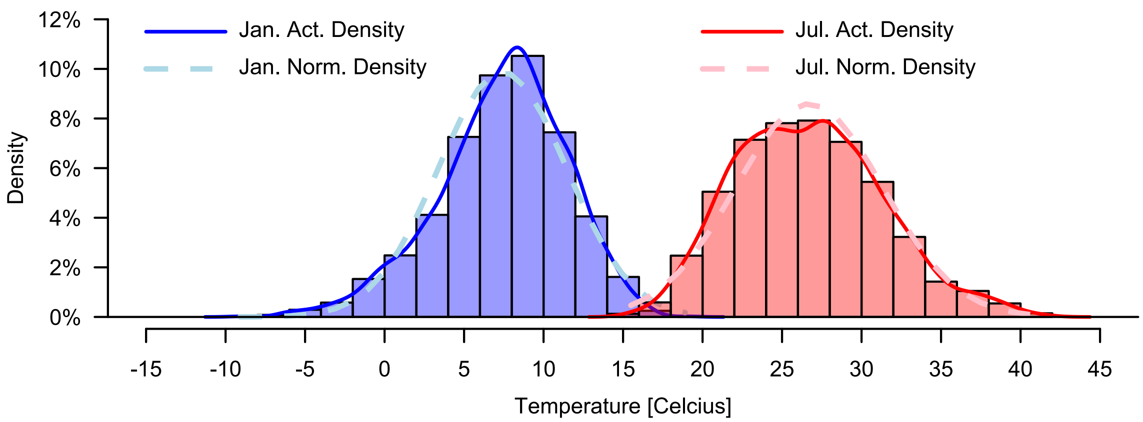

Figure 6 Historical high temperatures for January and July

To generate a pair of correlated random normal variables, y_1 and y_2, with known means, μ_1 and μ_2, variances, σ_1^2 and σ_2^2, and correlation, ρ, the following may be used (Rickert, 2016):

$$x_1 = \mathcal{N}(0,1) \qquad y_1 = \mu_1 + x_1\sigma_1$$

$$x_2 = \mathcal{N}(0,1) \qquad y_2 = \mu_2 + \sigma_2(x_1\rho + x_2\sqrt{1-\rho^2})$$

y_1 and y_2 are the simulated low and high temperatures for a given day and will have the desired means, variances, and correlations. However, it is still possible for the high and low temperature to be reversed (i.e. $y_1 > y_2$). Simply swapping the values, such that all smaller values of the pair are in one list and larger values are in the other, will increase the correlation. Through simulation, this increase in correlation can be measured, and the ratio of the simulated correlation (ρ_s) and actual correlation (ρ) maybe used to correct for the artificial increase.

$$\rho' = \frac{\rho}{\left(\frac{\rho_s}{\rho}\right)} = \rho\left(\frac{\rho}{\rho_s}\right) = \frac{\rho^2}{\rho_s}$$

Using ρ' in place of ρ and swapping paired values, as described above, results in a paired list of high and low temperatures with correlation ρ. Monthly trends from Portland's historical data are shown in Table 7, with both the observed correlation from the data (ρ) and corrected correlation (ρ') used for simulation. Unfortunately, these calculated means would be low if used for future predictions. Within the data set used in this analysis, there is a statistically significant positive slope for average high and average low temperatures of 0.01591 and 0.0228, respectively. For standard deviations, the slopes are statistically insignificant. Equations for the increase in mean highs and lows, compared to the aggregated historical averages, are given below, where y is the current year.

$$\Delta_{t_{lo}} = 0.0228y - 45.1480 \qquad \Delta_{t_{hi}} = 0.0159y - 31.4535$$

Table 7 Historical monthly high and low temperatures (°C) and correlation factors

Month	**High Temperature**		**Low Temperature**		**Correlation**	
	Mean	*Std. Dev.*	*Mean*	*Std. Dev.*	*Observed*	*Corrected*
January	7.41	4.04	1.19	4.12	0.788	0.782
February	10.34	3.61	2.31	3.52	0.534	0.523
March	13.08	3.76	3.70	2.98	0.243	0.225
April	16.09	4.36	5.64	2.77	0.285	0.271
May	19.80	4.99	8.76	2.70	0.390	0.377
June	22.82	4.82	11.68	2.31	0.418	0.409
July	26.70	4.64	13.84	2.11	0.422	0.420
August	26.69	4.53	13.95	2.21	0.286	0.282
September	23.92	4.79	11.26	2.82	0.169	0.158
October	17.61	4.10	7.59	3.23	0.286	0.269
November	11.40	3.50	4.25	3.84	0.639	0.629
December	7.80	3.65	1.90	3.77	0.775	0.769

The probabilities that the average daily and 8:00 AM temperatures are less than 0°C is important to the calculations of precipitation; as such, the increases are also important for future predictions. For any normally distributed variable, X, multiplied by a constant, c, the resulting distribution cX is also normal with mean, $c\mu$, and variance, $c^2\sigma^2$.

$$X \sim \mathcal{N}(\mu, \sigma^2) \qquad\qquad cX \sim \mathcal{N}(c\mu, c^2\sigma^2)$$

In addition, the sum of any two normally distributed variables, X and Y, with means, μ_1 and μ_2, variances, σ_1^2 and σ_2^2, and correlation, ρ, will also be normal.

$$X + Y \sim \mathcal{N}(\mu_1 + \mu_2, \sigma_1^2 + \sigma_2^2 + 2\rho\sigma_1\sigma_2)$$

For average daily temperature, the distribution of average temperature may be found by averaging the distributions of high and low temperatures. Given means, μ_1 and μ_2, variances, σ_1^2 and σ_2^2, and correlation, ρ, the distribution of the average daily temperature will be:

$$\mathcal{N}\left(\frac{\mu_1}{2} + \frac{\mu_2}{2}, \frac{\sigma_1^2}{2^2} + \frac{\sigma_2^2}{2^2} + 2\rho\left(\frac{\sigma_1}{2}\right)\left(\frac{\sigma_2}{2}\right)\right) = \mathcal{N}\left(\frac{\mu_1+\mu_2}{2}, \frac{\sigma_1^2+\sigma_2^2}{2^2} + \frac{\rho\sigma_1\sigma_2}{2}\right)$$

The probability that the average daily temperature is less than 0°C may be directly calculated for this normal distribution. This section presents the general statistical framework to analyze temperatures. In the specific application and case study, at 8:00 AM (worst case scenario), the probability is based only on the distribution of low temperatures.

4.2 MODELING PRECIPITATION DATA AND DISTRIBUTIONS

Many regions have systems to measure rainfall. Often, the amount of rain per day and the amount of snow per day are included. For precipitation generally in the US, 13 inches (33 cm) of snow equals one inch of precipitation. This conversion allows for total precipitation per day to be calculated. The same data weather data set for Portland, OR, provided historical rain and snow measurements, which were combined.

Table 8 shows the estimates for the mean and variance of precipitation on days with rainfall, and the calculated percent of days without rainfall for each month.

Table 8 Monthly rain statistics and probability of days with no rain

Month	Probability of Zero Precip. on a Given Day	Daily Precip. Rate [Rate > 0 mm]	
		Mean	*Variance*
January	32.6%	7.7	77.1
February	36.6%	6.4	59.2
March	35.3%	5.6	35.5
April	42.0%	4.2	21.7
May	54.0%	4.7	30.1
June	64.6%	4.4	28.8
July	86.6%	3.7	22.8
August	83.8%	4.6	34.7
September	72.8%	5.6	55.9
October	52.7%	6.5	61.6
November	32.7%	7.7	83.2
December	31.4%	8.0	81.9

As with temperature, precipitation may be aggregated by month to account for monthly variation and sub-divided into two distributions: Bernoulli probability of precipitation versus no precipitation, and a Gamma distribution for the quantity of rain, given some rainfall (Li, et al., 2013). Given the daily average, μ, and daily variation, σ^2, of rainfall, the gamma parameters, α and β may be calculated directly.

$$\alpha = \frac{\mu^2}{\sigma^2} \qquad \beta = \frac{\mu}{\sigma^2}$$

A scalar constant applied to a Gamma distribution is still Gamma. For an hourly distribution, α would remain the same, but the rate parameter, β, would be multiplied by 24. To separate precipitation into rainfall and snow, the current temperature is needed. The correlated pair of high and low temperatures for the study period are used in combination with the mean correction factor.

For example, there is a 9.2% probability that the average daily temperature in January 2020 will be less than 0°C and a 32.6% probability of no rain. As such, the probability of snow is 6.2%, which corresponds to an average of 1.9 snowy days in January. However, during 8:00 AM, there is a 30.5% probability temperatures are below 0°C in 2020. Given the same probability of some rain, there is a 20.6% probability of snow during that hour, which corresponds to 6.4 mornings with some snow.

4.3 MODELING WIND DATA AND DISTRIBUTIONS

A key factor that influences aviation performance is wind, and drones are highly susceptible due to their limited power and weight. The distribution of wind speeds may be modeled using a variety of known probability distributions with the Weibull ranking among the best (Qin, et al.,

2011); however, many models have been shown to be adequate. The creation of wind models is dependent on both the amount of historical data and the temporal granularity. For example, the inclusion of only a daily mean will not be enough to define most parametric models. A generalized understanding of wind effects does not require the accuracy of many climate models. As such, the choice of a probability distribution should be based on what can provide a reasonable approximation based on available data (NOAA, 2019).
There are long time series for Portland wind data, including historical average speeds, maximum gusts, percent calm, and direction. Gradient descent optimization was employed to find distribution parameters that provided reasonable approximations of historical trends. In Portland, different times of the year have different distributions of wind, which will directly influence failure odds. The distribution of wind speeds over a year is given in Figure 7.

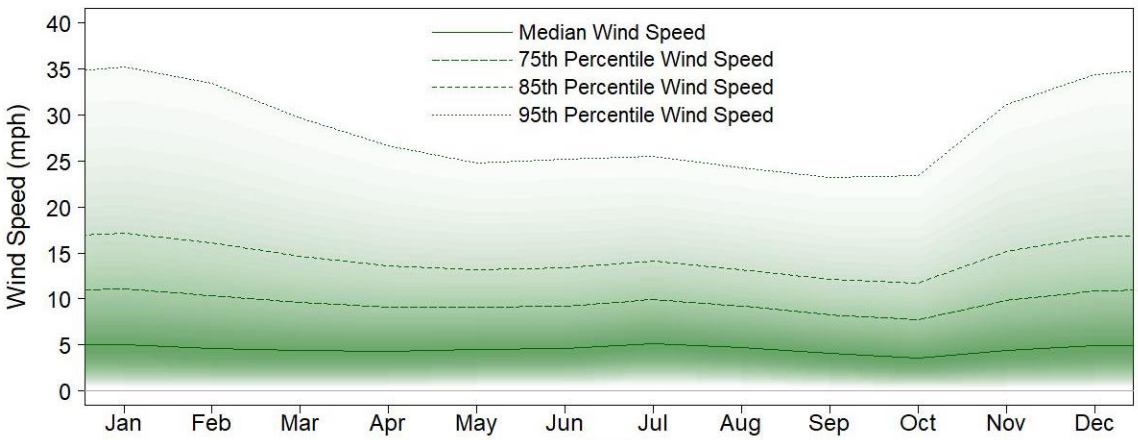

Figure 7 Simulated mean and confidence interval of wind speed in Portland, OR

Wind direction is also important. In Portland, winds mostly blow in the ESE direction during the winter months and the NW direction during the summer months (see Figure 8). This factor is important for determining a drone’s range at different times of the year. In January, areas to the NW of a depot will be restricted by a headwind, while the opposite is true in July.

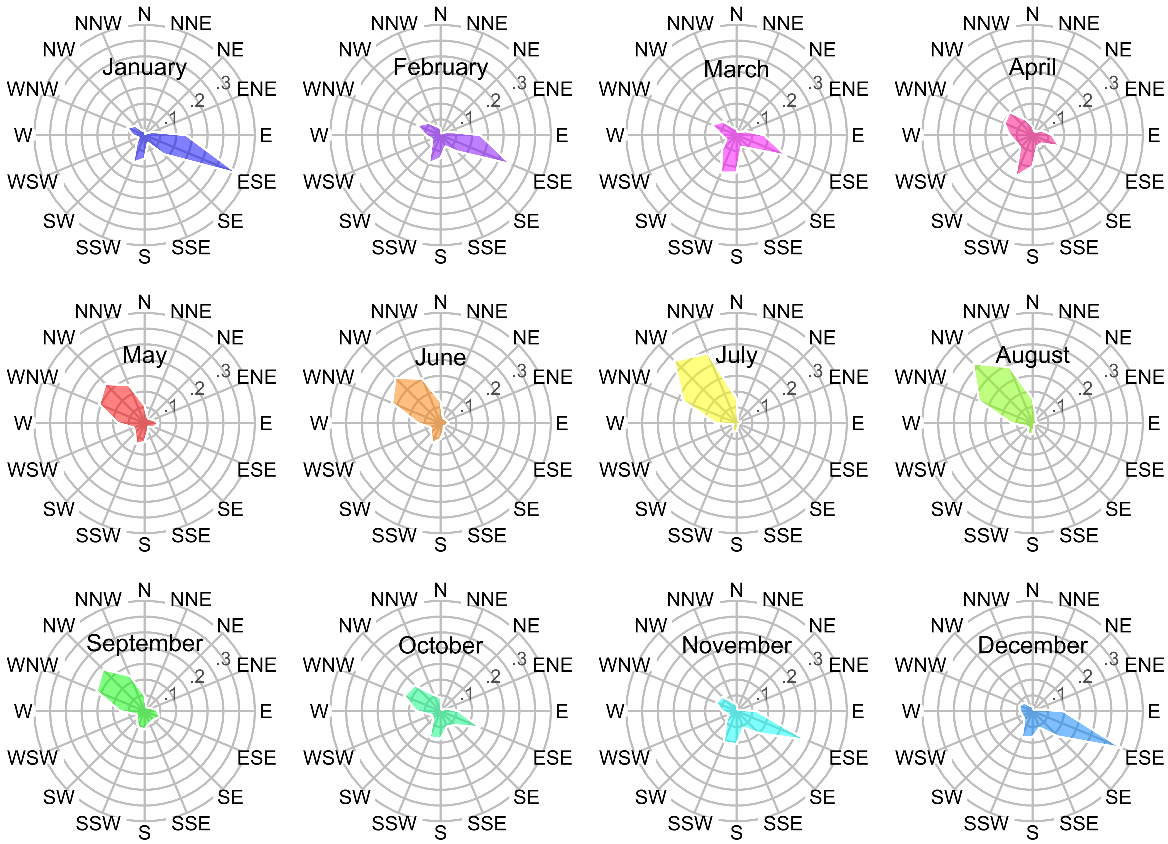

Figure 8 Probability of wind direction for each month in Portland, OR

5.0 RANGE RELIABILITY MODELING

Range is a key feature of drones that affects their cost as well as their competitiveness as a transportation mode. This section discusses how range is affected by wind, precipitation, and temperature.

5.1 MODELING RANGE

The range of a drone is determined by its weight, flying efficiency, and battery capacity. For applications with a central hub, this range is half of the distance a drone can travel, as a return trip must be accommodated. The following gives the energy necessary for level flight (Figliozzi, 2017):

$$p_l(t) = \frac{(m_t + m_b + m_l)g}{\vartheta(s)\eta_p} \; d \text{ [unitless} < 1] \tag{1}$$

where:

$$\begin{aligned}
p_l &= \text{power required for level flight [watts]},\\
t &= \text{travel time [seconds]} = (d/s),\\
m_b &= \text{drone battery mass [kg]},\\
m_l &= \text{drone load (defibrillator) mass [kg]},\\
m_t &= \text{drone mass tare (i.e. without battery and load) [kg]},\\
d &= \text{travel distance [m]},\\
\vartheta(s) &= \text{lift : to : drag ratio, or } (L/D) \text{ [unitless]},\\
s &= \text{travel speed [m], and}\\
\eta_p &= \text{total drone power transfer efficiency.}
\end{aligned}$$

From (1) it is possible to observe that energy consumption is directly proportional to drone mass and travel time and distance. The range estimations of this research consider the defibrillator 1.1 kg (2.4 lb) payload.

5.2 MODELING THE IMPACT OF TEMPERATURE

Temperature can have a significant impact on drone performance because drone lithium-ion batteries show optimal performance at approximately 20°C (68°F) but perform significantly worse at lower temperatures (see Figure 9). For lithium batteries, the output voltage is dependent on its operating temperature (Samadani, 2015). In this study, battery available energy or capacity is assumed to decrease following a parabolic curve. The maximum (100%) will be at 20°C (68°F) and the minimum (50%) at -20°C (-4°F). At higher temperatures, the capacity decreases linearly from 100% to 95% from 20°C (68°F) to 55°C (131°F). Battery makers recommend no operation outside this temperature range (Alibaba, 2019).

$$capacity = \begin{cases} -0.0003125t^2 + 0.0125t + 0.875 & -20 < t < 20 \\ 1 - .05\left(\frac{t-20}{55-20}\right) & 20 \leq t < 55 \\ 0 & otherwise \end{cases}$$

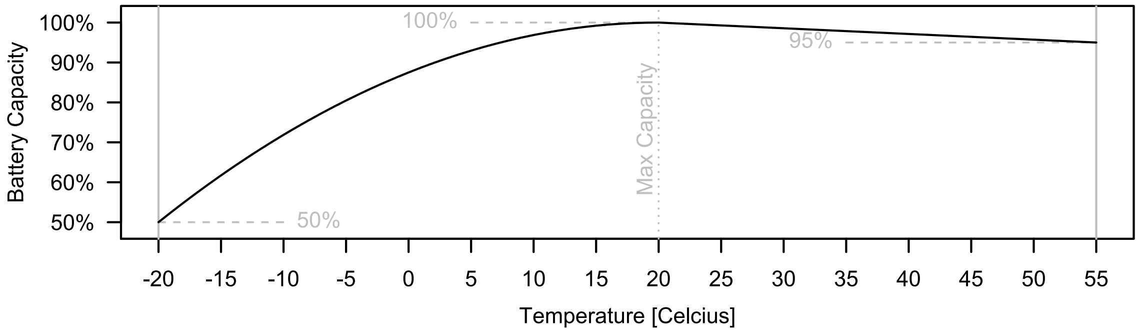

Figure 9 Battery capacity versus temperature and equations

In addition, battery capacity degrades linearly with the number of cycles up to a point. Often, the degradation accelerates when a battery reaches 80% of optimal capacity. At this point, the battery is considered unreliable and no longer used. Prior to this point, the battery will have above 80% optimal capacity, but the exact amount will be unknown for any specific trip. As such, a random uniform distribution from 0.8 to 1.0 may be used in association with temperature for simulation to define the initial condition of the battery with an assumption that faulty or unreliable batteries will not be used.

OHCA events are more frequent during the 8:00 AM hour, which is typically the coldest hour of the day. As such, only the distribution of low temperatures is needed in this study. Figure 10 shows the means and confidence intervals for daily high and low temperatures.

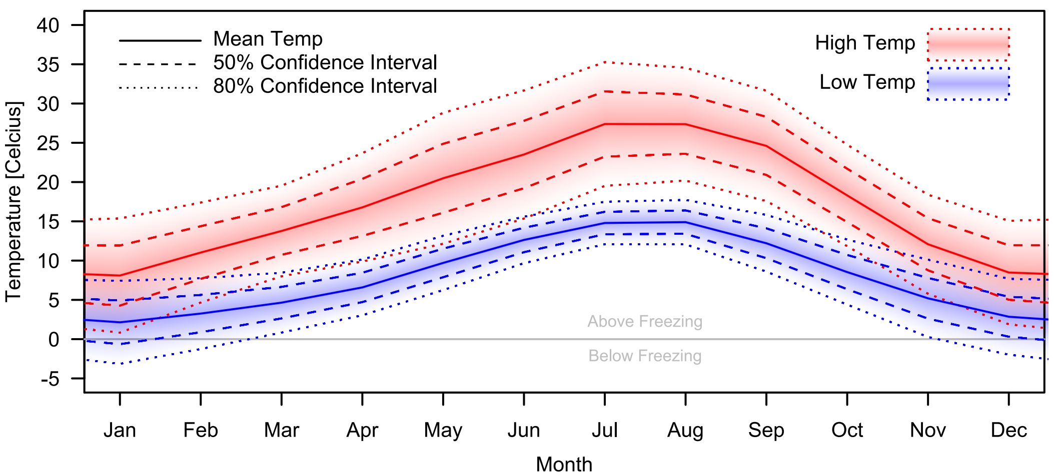

Figure 10 Means and confidence intervals for high and low temperatures by month

Figure 11 shows the probability of failure as a function of the total distance traveled, assuming an ideal 42-minute flight time. The left and right edges of the shaded regions are defined using distributions of the low and high temperatures, respectively. The purple area is based on the yearly average highs and lows, while the blue region represents the worst-case (i.e., coldest) temperatures in January. The potential range of a drone will be half of the total available flight distance, as return trips must be accommodated. The probability of failure is the percent of simulated trips that failed to reach a given range.

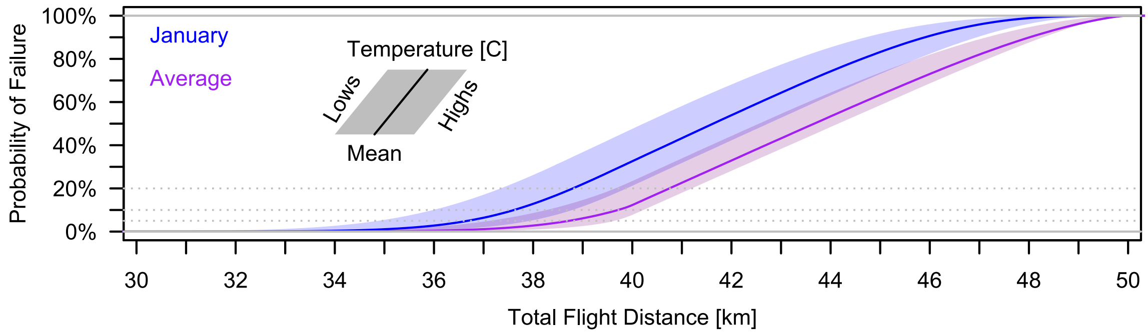

Figure 11 Failure probability due to temperature and battery charge vs. flight distance

Winter will have worst-case flight ranges as compared to the yearly averages. Yet, the range in the worst case is still larger than the maximum allowable due to time constraints for urgent medical deliveries. Even allowing for 14.5 minutes of flight time, the average ambulance arrival time in rural areas, more than 95% of drones will have enough battery for the 35 km (22 mi) trip, 17.5 km (11 mi) in each direction.

In addition, the available range corresponds to a large service area. The 3-minute delivery area covers 40 km^2 (15.7 mi^2), while 7 minutes (the urban ambulance average response time) allow for an area of 222 km^2 (86 mi^2). This is functionally the size of many cities. Based on Portland weather conditions, large cities would require just a few drone hubs for full coverage.

5.3 MODELING THE IMPACT OF PRECIPITATION

Many modern drones advertise some resistance to rain. As such, not all precipitations events would be considered failures. Considering rain alone (i.e., no snow), defining a specific cutoff for the permitted amount of rain would result in different failure odds. Figure 12 shows probability failure (plotted logarithmically) as a function of the maximum allowable precipitation rate. As an example, if drones are not sent during heavy rain, then drones will be unavailable (a failure condition) 4% of the time in January and <0.1% of the time in July.

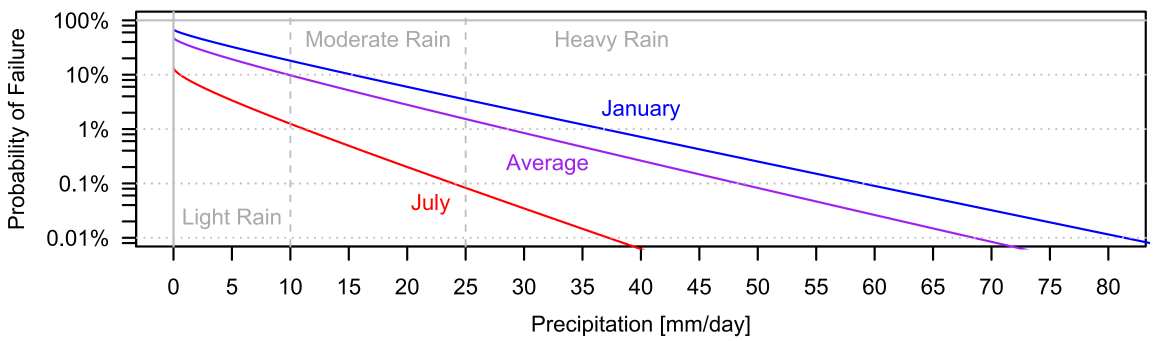

Figure 12 Probability of failure as a function of rainfall rate cutoff

Most drone manufacturers recommend not to fly drones during snowfalls. As such, all snowy weather would cause a failure condition. However, if the amount of snow is considered such that some snowfall is acceptable, the failure rates are also dependent on the precipitation cutoff (see Figure 13).

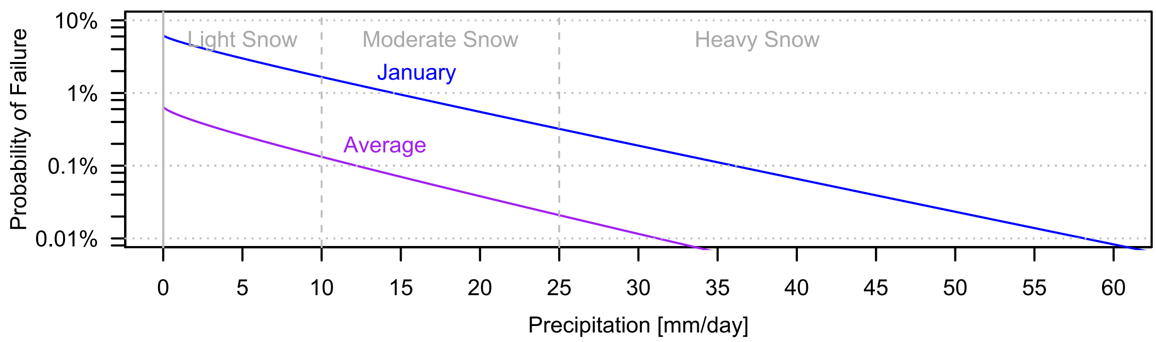

Figure 13 Probability of failure as a function of snowfall rate cutoff.

The cutoff points for snow and rain do not need to be equal. For example, if drones are permitted to fly in snow up to 10mm/day (light snow) and rain up to 25mm/day (light and moderate rain), then drones in January will be unavailable about 2% of the time due to snow and about 4% of the time due to rain.

5.4 MODELING THE IMPACT OF WIND

For winds, the worst case is a headwind where the flight path is directly against the wind's direction of travel. In the best case, the drone has an increased speed due to a tailwind. Given a wind bearing, its speed, and a drone's flight speed, an angle-side-side triangle is formed (Figure 14). This arrangement requires an algorithm to solve as there may be 0, 1, or 2 possible answers. The following algorithm may be used to solve for the fastest feasible flight path, if possible. It combines the law of cosines and solves for the unknown using the quadratic formula. s_w is wind speed, s_d is drone speed, and r_w is the angle between wind bearing and destination bearing.

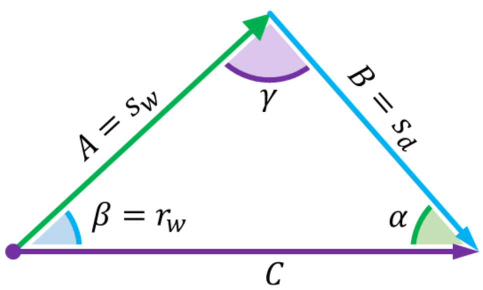

Figure 14 Setup and notation to solve an angle-side-side triangle.

Beginning with the law of cosines, where side A, side B, and angle β are known, but C is unknown. Solve for 0, then put in the quadratic form with C as the unknown.

$$B^2 = A^2 + C^2 - 2AC\cos(\beta)$$
$$0 = A^2 + C^2 - 2AC\cos(\beta) - B^2$$
$$= (1)C^2 + (-2A\cos(\beta))C + (A^2 - B^2)$$

Solve for C using the quadratic formula and simplify.

$$C = \frac{-(-2A\cos(\beta)) \pm \sqrt{(-2A\cos(\beta))^2 - 4(1)(A^2 - B^2)}}{2(1)}$$
$$= \frac{2A\cos(\beta) \pm 2\sqrt{A^2\cos^2(\beta) - (A^2 - B^2)}}{2}$$
$$= A\cos(\beta) \pm \sqrt{B^2 + A^2(\cos^2(\beta) - 1)}$$
$$= A\cos(\beta) \pm \sqrt{B^2 - A^2\sin^2(\beta)}$$

Mathematically, there are potentially two solutions, C_1 and C_2.

$$C_1 = A\cos(\beta) + \sqrt{B^2 - A^2\sin^2(\beta)}$$
$$C_2 = A\cos(\beta) - \sqrt{B^2 - A^2\sin^2(\beta)}$$

However, in the context of flight speed triangles, negative and imaginary solutions are not applicable, and the fastest speed is preferred. Given that $C_1 \geq C_2$ for real solutions, C_1 is used, given that the quantity under the square root is greater than 0.

As an example, assume a drone speed of 20mps, wind speed of 30mps, and a wind direction 30° away from the travel direction, both triangles in Figure 15 are valid solutions where the drone flies at a 20mps and is able to reach the destination. The key factor is the effective travel speeds and initial flight bearings. A drone using the initial travel bearing from the second triangle would reach its destination three times faster than a drone using the initial bearing from the first.

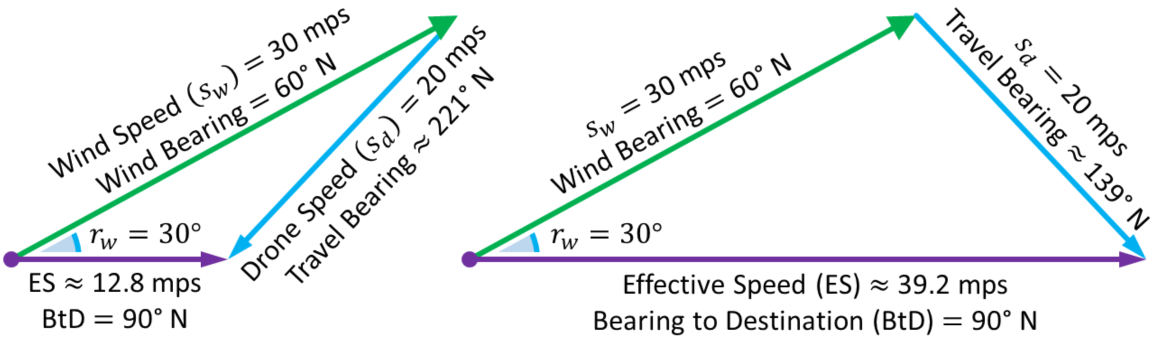

Figure 15 Two valid solutions to an angle-side-side triangle problem

For headwind and tailwind simulations, flight times are held constant for arbitrarily selected two-minute and ten-minute cases. For each trial, distance traveled within the time-limit is recorded. The probability of delivery failures due to wind was calculated based on the percent of trips that fail to reach a given distance within the allowable time. The shaded regions of Figure 16 and Figure 17 show a range of failure probabilities between a simulated headwind versus simulated tailwind and the result using a random bearing as the central line. As the flight time increases, the probability of failure also increases. In Figure 17, the y-axis of Figure 16 is transformed from linear to logarithmic.

At a 20% acceptable fail rate for 2-minute deliveries, the worst case for the range has decreased from 2.4 km (1.5 mi) to about 2 km (1.2 mi); a reduction of 16%. At a 5% acceptable failure rate, the range is further reduced to about 1.3 km (0.8 mi). While the theoretical range of drones is large (see Figure 11), the practical range for timely deliveries is a limiting factor. In Figure 17, the y-axis of Figure 16 is transformed from linear to logarithmic.

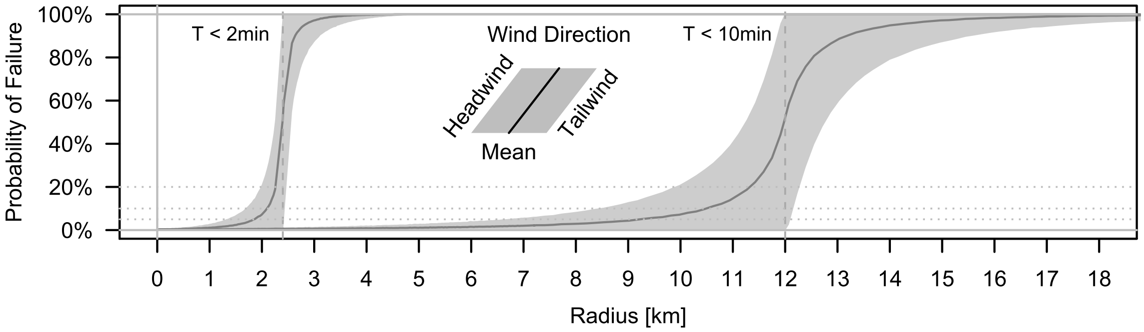

Figure 16 Probability of failure versus radius due to wind with linear y-axis

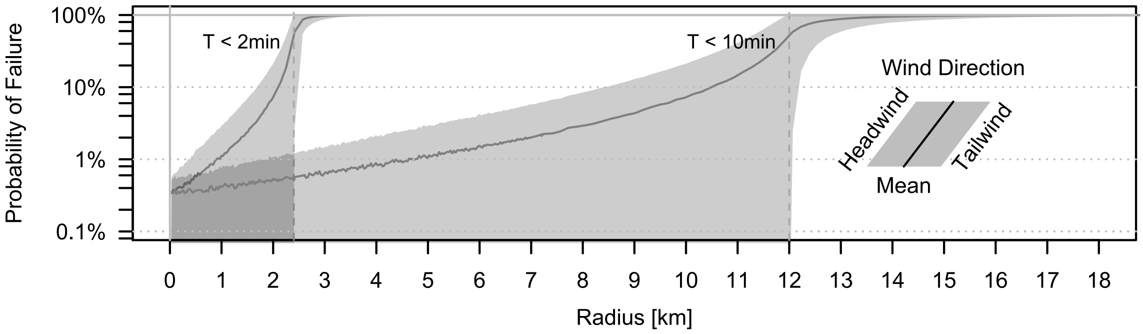

Figure 17 Probability of failure versus radius due to wind with logarithmic y-axis

Figure 17 shows that the average potential failure from wind is above 0.1% for a 2 minute or a 10-minute trip. Wind plays a key role in determining acceptable failure rates and for determining a potential range for drone deliveries. Notably, having multiple hubs will reduce failure rates from the wind as different hubs may be employed depending on wind direction. Headwinds and potential failure from one direction may be tailwinds and success from another.

6.0 ENERGY AND EMISSIONS MODELING

Drones can be the most efficient and sustainable mode of transportation under certain conditions. This section discusses the competitiveness of drones against ground vehicles: conventional vans with internal combustion engines (ICE), electric vans (EV), and new sidewalk and roadway autonomous delivery robots (SADR and RADR respectively). A formulation is proposed to compare different scenarios.

6.1 BACKGROUND

Vehicle electrification has also been studied as potential and cost-effective way to reduce urban freight emissions (Feng and Figliozzi, 2012; Lee et al., 2013; Davis and Figliozzi, 2013). Other studies (Jennings and Figliozzi, 2019 and 2020) analyzed the regulation and characteristics of sidewalk and road ADRs (respectively) in the USA and studied potential time and cost savings. When compared to a conventional human-driven delivery van, sidewalk ADRs can reduce cost, time, and vehicle travel in some instances. Road delivery robots are also more economical when delivery routes are relatively short. However, due to their limited range, vehicle miles tend to increase in most scenarios. The rate and speed of adoption of RADRs will greatly depend on costs and ease of entry into the delivery market as discussed by studies focusing on the adoption of autonomous trucks by freight organizations (Talebian and Mishra, 2018; Simpson et al. 2019).

Figliozzi (2017) derives analytical formulas to compare operational and lifecycle emissions and energy consumptions of drones, diesel van, electric vans, and tricycles. Figliozzi (2017) shows that it is possible to find emissions breakeven points as a function of customers in a route, efficiency of the vehicles, distance to customers, density of delivery area, and drone size/payload. Air drones are more CO_2 efficient for small payloads and single deliveries in rural areas but less efficient for large payloads or when many customers are grouped in dense urban areas. Drones consume less energy and emissions per package-km than delivery vans. Kirschstein (2020) provide a more detailed energy consumption model including takeoff, level flight, hovering, and landing; similar results were obtained, i.e. drones requires more energy in urban areas with high customer density and less energy in rural settings low customer density that trucks.

6.2 VEHICLE CHARACTERISTICS

ADRs are electric powered ground vehicles that can deliver items or packages to customers without the intervention of a delivery person. ADRs can be divided into two types. Sidewalk autonomous delivery robots (SADRs) are pedestrian sized robots that only utilize sidewalks or pedestrian paths. On-road or simply road autonomous delivery robots (RADRs) are vehicles that travel on roadways shared with conventional vehicles. ADRs use sensors and navigation technology that allow them to travel on roads and sidewalks without a driver or on-site delivery staff. The ground vehicles studied in this research have already been utilized in previous studies. Starship Technologies is producing the SADR that has been deployed in most locations and have received ample media coverage (Jennings and Figliozzi, 2019). Among the companies prototyping RADRs there are two that stand out: NURO and uDelv (Jennings and Figliozzi, 2020). The chosen high-performance drone, MD4-3000, has already been analyzed by Figliozzi (2017) where it was compared against the performance of tricycles, a typical delivery diesel van (Dodge RAM) utilized in the US, and an electric van (Renault Kangoo) utilized in Europe. The Dogde RAM is the only internal combustion engine (ICE) vehicle in Table 9.

Table 9 presents a summary of vehicle characteristics. The drone has the lowest tare and payload but the SADR has the lowest range and speed. The RADRs have less limitations regarding payload and range but these are still substantially lower than the payload and range of a conventional van. The electric van has relatively low energy consumption but reasonable performance in terms of payload and range for short and medium route lengths. SADRs have limited range and can be complemented by specialized vans usually called “mothership” vans, that can be utilized to drop off and pick up several SADRs. The mothership van is not an autonomous vehicle and requires a driver. Henceforward specialized vans that carry SADRs will be denoted simply as motherships. If SADRs are serving customers nearby, i.e. the service area is not far away, a mothership is not necessary which simplifies the operation of the sidewalk deliver robot and considerably reduces road distance traveled, energy consumption, and emissions. Unlike SADRs, even small RADRs are designed to share roadways with conventional motorized vehicles. Hence RADRs are not dependent on a mothership.

Table 9 - Key Vehicle Characteristics

Vehicle	Tare (kg)	Max. Speed (kph)	Payload (kg)	Range (km)	Energy consumption (wh/km)
Starship	18.1	6.4	18.1	6.4	24.7
Nuro	680	56	110	16.1	139.6
uDelv	1890	97	590	97	193.9
MD4-3000	10.2	72	5.0	36	21.6
Renault Kangoo EV	1300-1430	160	650-800	120*	205
Dodge RAM	2170	180	1890	695	1,016

* 120 km under extreme winter conditions, 199 km under temperate conditions

6.3 METHODOLOGY

In this section the methodology used for comparing the travel, energy, and emissions performance is presented. The methodology is based on continuous approximations. As indicated by Daganzo et al. (2012) these types of analytical approximations are appropriate to address big picture questions because they are parsimonious, tractable, and yet realistic when the main tradeoffs are included. This type of modeling approach has been successfully used in the past by many authors to model urban deliveries and logistic problems (Ansari et al., 2018).

6.3.1 Formulation

The constraints analyzed in this research include range, duration, capacity, and number of customers served. The notation used is presented below.

n = Number of stops or delivery locations

$m =$ Number of vehicles required to deliver to n customers

$a =$ Area (units length squared) of the service area (SA) where n customers reside

$\delta = n/a$, customer density

d = Service area to depot distance

R = Effective vehicle range

Q = Vehicle capacity in number of customers

$v =$ Average speed of the vehicle in the long haul

$v_l =$ Average speed of the vehicle in the local service area

$T =$ Maximum duration of shift or tour (same for all vehicle types)

$t_0 =$ Time to deliver at a customer including time to pick up a parcel

$t_u =$ Unload time

$t = t_0 + t_u =$ Total time vehicle is idle (i.e. not traveling) during a delivery

$k_l =$ Routing parameter

e = Energy consumption per unit distance (wh/km)

κ = Carbon emissions per unit of energy (CO_2 kg/wh)

$\varepsilon =$ ratio between store order size and delivery order size

By utilizing continuous approximations to estimate the average distance $l(n, m)$ traveled by a fleet of vehicles (Daganzo et al. (2012); Figliozzi, 2008) it is possible to write the following fleet size and route duration constrains, respectively:

$$m \geq \left\lceil \frac{k_l\sqrt{an}}{R-2d} \right\rceil$$

$$T \geq \left(\frac{2d}{v} + \frac{k_l}{mv_l}\sqrt{an}\right) + \frac{t\,n}{m}$$

It is assumed that all the vehicles depart the depot at the beginning of the time period T. Hence, the fleet size m is equal to the number of tours.

In some scenarios, the constraint is to serve a maximum number of customers n within the allowed time T with a given fleet size. For this purpose, a novel equation is developed. The equation that provides this number is obtained by solving for n. The result is the following expression:

$$n = \left\lfloor \frac{2\left(\tau - \frac{2d}{v}\right)\left(\frac{t}{m}\right) + \left(\frac{k_l\sqrt{a}}{mv_l}\right)^2}{2\left(\frac{t}{m}\right)^2} - \left(\frac{4\left(\tau - \frac{2d}{v}\right)\left(\frac{t}{m}\right)\left(\frac{k_l\sqrt{a}}{mv_l}\right)^2 + \left(\frac{k_l\sqrt{a}}{mv_l}\right)^4}{4\left(\frac{t}{m}\right)^4}\right)^{1/2} \right\rfloor$$

The floor function is used to avoid a fractional number of customers. The derivation of the formula is presented in the Appendix. The capacity constraint is simply stated as $m \geq \lceil n/Q \rceil$.

The above formulas assume that when several vehicles are utilized, $m > 1$, the service area is partitioned into homogenous areas as described by Daganzo (1984).

The energy consumed E and carbon emissions K produced by m vehicles are calculated utilizing the travel distance multiplied by the corresponding energy and emission factors for each vehicle type with m that satisfy the range, capacity, time, and number of delivery constraints.

$$K = \kappa \ E \ = \kappa \ e \ \left(2dm + k_l\sqrt{an}\right)$$

6.3.2 Data, Assumptions, and Scenario Design

Vehicle efficiencies are analyzed utilizing two approaches: (a) estimating efficiency of each vehicle when delivery area size, delivery time, and distance from the depot vary and (b) estimating the efficiency of the vehicles when customer density or number of deliveries change. In the latter approach the number of customers served varies from $n = 25$ to $n = 200$ and this interval includes the average number of package deliveries per conventional vehicle that is approximately 120. Vehicle specifications are drawn from manufacturer websites or press releases and parameters are representative of delivery conditions in urban and suburban areas

The Starship SADR is assumed herein because it complies with US regulation and it is the most extensively tested SADR at the time of this writing. The Starship SADR range is approximately 4 miles and a Starship is designed to carry up to three grocery bags or up to six small/medium packages – as a reference most Amazon packages parcels are less than five pounds or 2.3 kg (Forbes, 2019). SADRs are complemented by a mothership van. The mothership drop-offs or picks-up up to 8 SADRs per tour. The same formulas and constraints presented earlier in this section can be directly applied to the mothership but assuming that n represents the number of SADRs and that the capacity of the mothership is eight SADRs. When the depot is at the center of the SA ($d = 0$), a mothership is not utilized. The drone always services one customer at the time hence the calculations of energy and emissions are straightforward since customers are not grouped in routes and distances are estimated as the crow flies (i.e. Euclidian). For ground vehicles, the Manhattan metric is assumed which is reflected in the value of the routing parameter k_l.

The energy consumption coefficient per unit distance, denoted e, for each vehicle was estimated utilizing available battery and range information for the vehicles or manufacturers data. The values assumed for SADRs and RADRs are reasonable also according to other studies analyzing small ground robot energy consumption, for example Broderick et al. (2014). The following values are utilized in the numerical analysis: SADRs consume 24.7 wh/km, NUROs consume 140 wh/km, uDelvs consume 194 wh/km, electric vans (E-vans) consume 205 wh/km, and the electric mothership consume of 427 wh/km (currently the mothership can use a conventional internal combustion engine but an electric engine is assumed to facilitate future comparisons). The E-van and conventional ICE van values were obtained from the performance of the electric Renault Kangoo van and Dodge RAM (Figliozzi, 2017). The value for the mothership is obtained from the Mercedes Benz Sprinter cargo van that was modified to accommodate the SADRs shown in Figure 1 and assuming that the mothership utilizes an electric engine.

Urban areas are complex environments for autonomous vehicles with many deliveries/stops and interactions with pedestrians and cyclists. Hence, it is likely that autonomous vehicles will be designed with high safety standards and would require extra time to park, unload/load, and avoid conflicts with pedestrians and/or cyclists. Hence additional minutes and a lower average speed are assumed for autonomous vehicles. The following average delivery times t per customer are assumed: five minutes for autonomous SADRs, Nuros, Udelvs, and drone; 3 minutes for the E-van and conventional van with a driver. The following average local or service area speeds v_l are assumed: SADR: 2 km/h, Nuro and Udelv 10 km/h, and mothership or E-van 20 km/h. For the long-haul segment connecting the depot and the service area an average speed of $v = 40$ km/h is assumed.

7.0 ENERGY CONSUMPTION RESULTS

There are large differences among SADRs, RADRs, drones and EV/conventional vans in terms of capabilities. Hence, for a few combinations of parameters some vehicles cannot be feasibly deployed due to range, capacity, or time constraints. When it is not feasible to deploy a vehicle a table cell is filled out with “NA” which stands for “Not Available”. It should be noted that continuous approximations work best when the number of customers per vehicle is four or higher (Daganzo, 1984). In the scenarios presented only the SADR may serve less than four customers per vehicle and when this is the case the value has an accompanying asterisk and note in the corresponding table. However, it is important to point out that when this is the case the SADR is already not the most efficient vehicle and the value in the table is slightly underestimating the energy consumed per customer and the general trends and insights are not affected.

7.1.1 One vehicle efficiency

The first set of results study the efficiency of each vehicle varying key parameters such as delivery area size, distance to depot, and delivery time window. One vehicle of each type is deployed and energy consumption efficiencies are compared across vehicles. The baseline scenario assumes a service area $a = 1$ km^2, a depot at the center of the service area ($d = 0$), and a delivery time window $T = 8$ hours. The number of customers is estimated utilizing equation (3).

7.1.2 Service Area (SA)

Table 10 reports the results in terms of energy consumption per customer served as service area increases from $a = 1$ km^2 to $a = 30$ km^2. It is assumed that the depot is at the center of the SA ($d = 0$) and service time is $T = 8$ hours. A different color and bold are utilized to pinpoint the lowest value per row. The SADR is most energy efficient option for smaller service areas because a SADR can serve multiple customers (up to six) and have a low energy consumption per unit distance. The drone becomes the most energy efficient for large service areas (i.e. low-density scenarios) where the SADR serves less than six customers per vehicle.

Table 10 Impact of a on Energy Consumption per Customer (wh/customer)

Service Area a (in km^2)	Vehicle Type				
	SADR	NURO	Udelv	E-van	Drone
1	**10**	23	22	16	16
10	**38**	82	79	56	51
20	*76	168	120	84	**73**
30	*131	247	155	106	**89**

* Three or less customers per SADR

7.1.3 Depot - Service Area Distance

Table 11 reports the results in terms of energy consumption per customer served as depot-SA distance increases from $d = 0$ km to $d = 10$ kms. It is assumed that the service area is constant and equal to $a = 1$ km^2 and service time is $T = 8$ hours. The E-van is the most efficient vehicle when the depot is not at the center of the service area. Since SADRs are severely range constrained they must be complemented by a mothership even for relatively low d values. Hence, the SADR is less efficient than all the other ground delivery vehicles when a mothership must be utilized (even assuming an electric powered mothership).

Table 11 Impact of d on Energy Consumption per Customer (wh/customer)

Distance Depot – SA d (in kms)	Vehicle Type				
	SADR+ MS*	NURO	Udelv	E-van	Drone
0.0	**3**	23	22	16	16
2.5	72	42	36	**24**	124
5.0	117	61	51	**31**	232
7.5	161	NA	66	**39**	340
10.0	206	NA	81	**47**	448

* Mothership not utilized when $d = 0.0$

7.1.4 Delivery Time Duration

Table 12 reports the results in terms of energy consumption per customer served as delivery time duration decreases from $T = 8$ hours to $T = 1/2$ hour. It is assumed that the service area is constant and equal to $a = 1$ km^2 and distance $d = 0$ km. A different pattern emerges from previous results. The SADR is the most efficient vehicle until the duration of the delivery time window is $T = 2$ hours. For smaller values of T the SADR is too slow to feasibly deliver in a limited time frame. Given the low average travel speed of SADRs, 2 km/h in sidewalks, it is not possible to deliver to customers in a ½ time frame taking into account travel time and service time. The other ground vehicles also see a reduction of efficiency as the delivery duration decreases since it reduces the number of feasible deliveries according to equation (3). The drone becomes most efficient when delivery durations are short and fewer customers can be grouped in the route of a ground vehicle.

Table 12 Impact of T on Energy Consumption per Customer

Time to deliver T (in hours)	Vehicle Type				
	SADR	NURO	Udelv	E-van	Drone
8	**10**	23	22	16	16
4	**10**	23	32	24	16
2	**10**	34	47	34	16
1	*17	51	71	50	**16**
0.5	NA	78	109	75	**16**

* Three or less customers per SADR

7.1.5 Fleet Efficiency to Serve n Customers

The second set of results study the efficiency a fleet of vehicles that must service n customers. More than one vehicle of each type may be deployed to meet capacity, time, or range constraints. The baseline scenario assumes a service area $a = 1$ km^2, a depot service area distance $d = 2.5$ kms, and a delivery time window $T = 8$ hours.

Table 13 reports the results in terms of energy consumption per customer served as the number of customers served increases from $n = 25$ to $n = 200$. More than one vehicle of each type may be deployed to satisfy the range, capacity, or time constraints. The energy efficiency of all the ground vehicles increases when the number of deliveries or the delivery density increases as routes become more efficient by including more customers per vehicle. However, efficiency is reduced when more vehicles are required. For $n = 25$ to $n = 100$ NURO and Udelv are most efficient but the electric van is the most efficient vehicle for $n = 200$.

Table 13 Impact of n on Energy Consumption per Customer

Customers Served (n)	Vehicle Type				
	SADR+ MS	NURO	Udelv	E-van	Drone
25	127	**55**	76	81	124
50	114	47	**46**	49	124
100	84	34	**29**	30	124
200	67	31	23	**19**	124

8.0 DISTANCE AND EMISSIONS RESULTS

Changes in commercial vehicle on-road distance traveled are important to analyze autonomous delivery vehicles potential safety impacts and congestion relief. This section delves into topics related to drone competitive advantage in terms of delivery distance traveled and carbon emissions.

8.1 DISTANCE TRAVELED

Table 14 shows the distance traveled by the different vehicles per customer served as the number of customers served increases from $n = 25$ to $n = 200$. The baseline scenario assumes area size $a = 1$ km^2, distance $d = 2.5$ km, and $T = 8$ hours.

When comparing values, it is important to highlight that drones do not share the roads used by all the other ground vehicles. However, even for relatively short distances between the depot and the service area, drones travel a significantly longer distance and this is related to the inefficiency of their routes that only accommodate one customer per round trip from the depot.

SADRs travel on the sidewalk and the mothership travels on the road, hence, the distance for these two complementary vehicles are disaggregated. It was shown that SADRs can be energy efficient when delivering from the depot and without a mothership. Table 7 shows that when a mothership is utilized to carry the SADRs there could be an increase of both on-road and sidewalk travel when comparing against the other ground vehicles. There is a clear increase of MS on-road vehicle travel for $n \geq 50$. RADRs and the E-van have the same on-road distance traveled as long as the necessary fleets have the same size. RADRs could be more energy efficient for lower values of n but generate more miles and potentially more congestion when more vehicles are needed. Regarding safety and crashes, the NURO is smaller and designed to collapse and reduce damage in case of crashes (Verger, 2018). Future research efforts should analyze in detail potential externalities and conflicts with pedestrians caused by SADR travel on sidewalks.

Potential congestion impacts of RADRs are also a function of their size, the uDelv is similar in size to the E-van; however, the NURO is considerably smaller, roughly ½ the size of a small E-van and likely to contribute less to congestion on a per unit distance traveled basis. Regarding motherships, it is important to highlight that the Mercedes Benz Sprinter van, which is used as a prototype to carry the eight SADRs, is 70% and 130% longer than the Udelv and NURO vehicles respectively. Regarding vehicle width, which is important for parking in congested areas, two and ½ NUROs can potentially occupy the same parking space utilized by one mothership van. Considering that the mothership van may require additional space to unload and load the SADRs, SADRs may not be efficient in terms of curb utilization if a mothership is required.

Table 14 Per Customer Distance Traveled Varying n

Customers Served (n)	Vehicle Type					
	SADR*	MS	NURO	Udelv	E-van	Drone**
25	0.19	0.29	0.39	0.39	0.39	5.75
50	0.14	0.26	0.34	0.24	0.24	5.75
100	0.10	0.19	0.25	0.15	0.15	5.75
200	0.07	0.15	0.22	0.12	0.09	5.75

* sidewalk travel, ** air travel

8.2 CARBON EMISSIONS

Relative emissions by vehicle type can be easily estimated by taking into account that each unit of energy used by an ICE diesel vehicle generates 22.5 more CO_2 equivalent emissions than the emissions generated by using a similar unit of energy sourced from the electric grid in Oregon (Figliozzi, 2017). The 22.5 value may change with the electricity generation profile of each city or country, i.e. it is a function of the percentage of clean or dirty sources used, and the previous value is applicable to the state of Oregon in the US. The 22.5 value used in this research accounts for diesel vehicle emissions including well-to-tank (WTT) and tank-to-wheel (TTW) emissions.

The E-van consumes almost five times less energy per unit distance than the conventional ICE van (205 wh/km vs. 1016 wh/km) and including emissions then the E-van generates approximately 112 times less CO_2 emissions per unit distance traveled. Table 15 shows the carbon emissions of the electric vehicles as a percentage of the carbon emissions generated by the ICE Dodge RAM. It is clear that, regardless of the autonomous vehicle type utilized, the reduction in carbon emissions is always likely to be highly significant. On average, any autonomous vehicle emits less than 2% of the emissions emitted by utilizing an ICE diesel van. But as shown by the 0.9% emissions of the E-van, the main cause of this impressive reduction in emissions is the electrification of the engines.

Table 15 Per Customer CO2 Emissions Varying n – baseline ICE Van

Customers Served (n)	Vehicle Type				
	SADR+ MS	NURO	Udelv	E-van	Drone
25	1.4%	0.6%	0.8%	0.9%	1.4%
50	2.1%	0.9%	0.8%	0.9%	2.3%
100	2.5%	1.0%	0.8%	0.9%	3.7%
200	3.1%	1.4%	1.1%	0.9%	5.8%

The numbers in this table will be affected by the energy sources utilized to generate electricity. For example, in the US the national average CO_2 rate is 947.2 lbs/MWh but there is a high degree of variability across regions. The lowest rate is found in New York and upstate region (NYUP) with an average CO_2 rate of 253.1 lbs/MWh and the highest rate in the Mid-west region (MROE) with an average CO_2 rate of 1,678 lbs/MWh. In the NYUP region the main sources of electricity generation are hydro and nuclear (account for 66% of the total) whereas in the MROE region the main energy source is coal that accounts for 64% of the total generation (EPA, 2020). In the Pacific Norwest region, where Oregon is located, the average CO_2 rate of 639 lbs/MWh (EPA, 2020). Even assuming the dirtiest electricity generation profile in the US, CO2 emissions from a conventional van are several times higher than operational emissions from electric vehicles.

8.3 GROCERY STORE DELIVERY VS CUSTOMER DRIVING

Since electrification is a key factor to reduce carbon emissions, a question arises regarding the benefit of autonomous delivery vehicles when compared to the emissions of an electric and/or ICE passenger car. The issue of traffic generated when delivering from the supermarket or driving from home has been studied in the past (Cairns, 2005; Halldórsson et al., 2010) as well as the emissions reductions (Wygonik and Goodchild, 2012). It was concluded that with enough customers per route, supermarket delivery is more efficient than individuals driving to the store. However, previous research efforts did not include several key factors that affect the relative efficiency of store delivery vs customer driving to a store: (a) the growth of passenger EVs, (b) logistics sprawl, and (c) the number of items purchased and delivered.

In recent years there has been a growth of passenger electric vehicles in the US, mainly driven by the advent of the Tesla Model 3 (TM3). According to the EPA the energy efficiency of the TM3 is 28 kwh/100 miles or 174 wh per km (EPA, 2018); the TM3 is one of the most energy efficient passenger vehicles in the market. The Tesla Model 3 is now the most popular EV in the US and the third best-selling car in the state of California where the TM3 accounts for almost 60% of EV sales (Dow, 2020).

Urban logistics sprawl refers to increases in depot-service area distances, i.e. the relocation of depots away from customer locations. This phenomenon has been observed in many urban areas in different continents. Furthermore, the advent of e-grocery home delivery may increase distance delivery distances because delivery areas are not necessarily distributed around traditional industrial or wholesale land use areas (Keeling and Figliozzi, 2019). In this paper, higher levels of logistics sprawl are represented by higher values of d, the depot-service area distance. Next subsections analyze driving to store efficiency of ICE and EV vehicles with different levels of customer delivery density and logistics sprawl. It is assumed that a store is at the center of a circular delivery region of 1 km^2 and that customers can be served by an autonomous vehicle, E-van, conventional van, or drive to the store. Customers are distributed uniformly across the circular region. The delivery depot can be located at the store ($d = 0$) or at a distance $d = 2.5$ or $d = 10$ kms to simulate logistics sprawl.

The relative efficiency of driving to the store vs store delivery is a function of the number of products purchased at the store or delivered to each customer. Previous studies in multiple countries have shown that the mean number of products purchased in grocery trips is approximately nine with a long right tail that reaches up to 60 products (Sorensen et al., 2017). The average number of items in an online grocery basket is likely to have a similar value (Suel et al., 2015) but the number of products purchased online is influenced by the structure of shipping fees. When free shipping is available after reaching a minimum shopping cart value, customers tend to take advantage of this pricing feature which increases average order size. Subscription services like Amazon prime incentivize more frequent and smaller orders since shipping is free (Belavine et al., 2017). To facilitate comparisons between customer store shopping and store delivery, the ratio ε between store order size and delivery order size for carbon emissions breakeven condition is estimated.

8.3.1 Breakeven Results for ICE Vehicles

The 2016 average fuel efficiency of vehicles in the US was approximately 24.7 miles per gallon according to an EPA report (2017). Utilizing this ICE efficiency, the numbers in Table 16 can be interpreted as follows: to generate the same level of carbon emissions the store order size of a customer driving an ICE is 4,064 ($\varepsilon = 4064$) times larger than the order size delivered by a SADR when the depot is at the store ($d = 0$) and the SADR fleet delivers to $n = 25$ customers.

Given that the mean number of products purchased in grocery trips is approximately nine with a right tail of up to 60 products (Sorensen et al., 2017), deliveries utilizing any autonomous vehicle generate less emissions even with a long depot-delivery area distance. On the other hand, delivering with a conventional van could be more environmentally friendly only when the depot is at or close to the store and many customers are served (large n). Bold and a different color are utilized to highlight when delivering from the store is more efficient assuming an average order size of nine products.

Table 16 ICE Order Size Ratio ε for CO2 Breakeven Condition

Distance Depot – SA (in kms)	Customers Served (n)	Vehicle Type					
		SADR +MS*	NURO	Udelv	E-van	Drone	Conv. Van
$d = 0$	25	**4,064**	**718**	**517**	**489**	**1,197**	4.4
	50	**5,748**	**1,016**	**731**	**692**	**1,197**	6.2
	100	**8,129**	**1,436**	**1,034**	**978**	**1,197**	8.8
	200	**11,496**	**2,031**	**1,462**	**1,383**	**1,197**	**12.4**
$d = 2.5$	25	**153**	**354**	**255**	**241**	**157**	2.2
	50	**171**	**413**	**423**	**400**	**157**	3.6
	100	**233**	**564**	**682**	**645**	**157**	5.8
	200	**290**	**637**	**846**	**1,014**	**157**	**9.1**
$d = 10$	25	**51**	**140**	**101**	**95**	**43**	0.9
	50	**53**	**149**	**187**	**177**	**43**	1.6
	100	**71**	**200**	**338**	**319**	**43**	2.9
	200	**86**	**208**	**373**	**563**	**43**	5.0

* MS required when $d > 0$
Bold when delivering from the store is more efficient

8.3.2 Breakeven Results for Tesla 3 EV

Table 17 shows the breakeven order size ε when a customer drives to the store utilizing a Tesla model 3. Given that the mean number of products purchased in grocery trips is approximately nine with a right tail of up to 60 products (Sorensen et al., 2017), deliveries utilizing a conventional van are no longer more environmentally friendly.

Even electric autonomous vehicles may not be more environmentally friendly than a TM3 when there is logistics sprawl ($d > 0.0$). With free shipping and small order sizes, customers ordering 1 or 2 items per delivery, driving a TM3 to the store is on average more environmentally friendly than home delivery. Hence, it is not self-evident anymore that store delivery is more environmentally friendly than driving to the store unless all the key factors are stated: delivery vehicle type, customer vehicle type, depot-service area distance, in-store order size, and delivery order size. Bold and a different color are utilized to highlight when delivering from the store is more efficient assuming an average order size of nine products.

Table 17 Tesla 3S Ratio Order Size Ratio ε for CO2 Breakeven Condition

Distance Depot – SA (in kms)	**Customers Served (n)**	**Vehicle Type**					
		SADR +MS*	**NURO**	**Udelv**	**E-van**	**Drone**	**Conv. Van**
$d = 0$	25	35	6	4	4	**10**	0.04
	50	49	9	6	6	**10**	0.05
	100	69	**12**	**9**	8	**10**	0.07
	200	98	**17**	**12**	**12**	**10**	0.11
$d = 2.5$	25	1.3	3.0	2.2	2.1	1.3	0.02
	50	1.5	3.5	3.6	3.4	1.3	0.03
	100	2.0	4.8	5.8	5.5	1.3	0.05
	200	2.5	5.4	7.2	8.7	1.3	0.08
$d = 10$	25	0.4	1.2	0.9	0.8	0.4	0.01
	50	0.4	1.3	1.6	1.5	0.4	0.01
	100	0.6	1.7	2.9	2.7	0.4	0.02
	200	0.7	1.8	3.2	4.8	0.4	0.04

* MS required when $d > 0$
Bold when delivering from the store is more efficient

9.0 CONCLUSIONS

Growing e-commerce volumes and consumer expectations of free and faster shipping are pushing the adoption of new delivery vehicles. For the delivery of time-sensitive supplies, drones may provide the means to bypass many obstacles experienced by ground transportation vehicles. However, drones are subject to their own set of constraints that limit the likelihood of successful deliveries.

The number of drones needed is highly dependent on charge times, use of battery swapping, and population in the service area. Additional consideration should also be given to potential mechanical failures and maintenance schedules. It is important to note that failure due to extreme weather conditions cannot be addressed by simply having more available drones. Extreme weather conditions, which will result in a failed delivery for one drone, will result in a failed delivery for any other drone because drones cannot operate under extreme weather conditions. Wind is a key constraint for drone deliveries. Successful drone deliveries are highly influenced by wind speeds, wind direction, and precipitation rates; however, the ambient temperature may mostly be ignored for short and strict delivery times limits.

Furthermore, there is an access and equity question associated with a drone's ability to deliver to some areas. For example, airports are often restricted flight zones that allow for no drone operations. Such areas are also areas with higher proportions of lower-income communities. Future research could examine where a delivery system could be employed and what ground delivery systems are required locally to adjust for access differences.

In terms of energy and emissions efficiency there is no vehicle type that dominates across the board. Drones are more efficient in time constrained and low-density delivery scenarios. Road autonomous delivery robots (RADRs) are more efficient than E-vans when delivering to relatively low number of customers. New air and ground autonomous vehicle types may reduce carbon emissions significantly but they may not necessarily reduce on-road travel. For some autonomous vehicles the reduction of on-road travel is also accompanied by additional travel on sidewalks (SADRs) or air travel (drones).

ACKNOWLEDGEMENTS

Travis Glick, Avinash Unnikrishnan, Katherine Keeling, and Jeff Broderick are acknowledged for their contribution to different parts of this report and related research papers.

10.0 REFERENCES

Alibaba, 2019. 36v 10ah lipo battery. [Online]
Available at: https://www.alibaba.com/product-detail/36v-10ah-lipo-battery-for-e_60444386060.html
[Accessed 2019].

Allen, J., Piecyk, M., Piotrowska, M., McLeod, F., Cherrett, T., Ghali, K., Nguyen, T., Bektas, T., Bates, O., Friday, A., Wise, S. and Austwick, M. (2018). Understanding the impact of e-commerce on last-mile light goods vehicle activity in urban areas: The case of London. Transportation Research Part D: Transport and Environment, 61, pp.325-338

American Heart Association, 2018. Heart Disease and Stroke Statistics - 2018 Update: A Report From the American Heart Association. Circulation, 137(12).

Aniwaa, 2019. MD4-3000 Microdrones. [Online]
Available at: https://www.aniwaa.com/product/drones/microdrones-md4-3000/
[Accessed 2019].

Ansari, S., Başdere, M., Li, X., Ouyang, Y. and Smilowitz, K., 2018. Advancements in Continuous Approximation Models for Logistics and Transportation Systems: 1996–2016. Transportation Research Part B: Methodological, 107, pp.229-252.

Appriss. (2020). Consumer returns in the retail industry 2019 [online]. Available at: https://appriss.com/retail/wp-content/uploads/sites/4/2020/01/AR3019-2019-Customer-Returns-in-the-Retail-Industry.pdf (Accessed 28 June 2020).

Amazon.com, Inc. (2018). Amazon Logistics [online]. Available at: https://logistics.amazon.com/ (Accessed: 30 June 2020).

Belavina, E., Girotra, K. and Kabra, A., 2017. Online grocery retail: Revenue models and environmental impact. Management Science, 63(6), pp.1781-1799.

Bernon, M., Cullen, J. and Gorst, J. (2016). Online retail returns management: Integration within an omni-channel distribution context. International Journal of Physical Distribution and Logistics Management, 46(6/7), pp. 584-605.

Boutilier, J.J., Brooks, S.C., Janmohamed, A., Byers, A., Buick, J.E., Zhan, C., Schoellig, A.P., Cheskes, S., Morrison, L.J., Chan, T.C.Y., 2017. Optimizing a Drone Network to Deliver Automated External Defibrillators. Circulation 135, 2454–2465. https://doi.org/10.1161/CIRCULATIONAHA.116.026318

Brooks, S. C. et al., 2010. Out-of-Hospital Cardiac Arrest Frequency and Survival: Evidence for Temporal Variability. Resuscitation: Official Journal of the European Resuscitation Council, 81(2), pp. 175-181.

Cairns, S., 2005. Delivering Supermarket Shopping: More or Less Traffic?. Transport Reviews, 25(1), pp.51-84.

Casella, G. & Berger, R. L., 2002. Statistical Inference. 2nd ed. Pacific Grove, CA: Daxbury.

Chan, P. S., Krumholz, H. M., Nichol, G. & Nallamothu, B. K., 2008. Delayed Time to Defibrillation after In-Hospital Cardiac Arrest. The New England Journal of Medicine, 358(1), pp. 9-17.

Chauhan, D., Unnikrishnan, A., Figliozzi, M., 2019. Maximum coverage capacitated facility location problem with range constrained drones. Transportation Research Part C: Emerging Technologies 99, 1–18. https://doi.org/10.1016/j.trc.2018.12.001

Chauhan, D.R., Unnikrishnan, A., Figliozzi, M., Boyles, S.D., 2020. Robust Maximum Coverage Facility Location Problem with Drones Considering Uncertainties in Battery Availability and Consumption. Transportation Research Record 036119812096809. https://doi.org/10.1177/0361198120968094

Chen, J., 2017. Rwanda has shown that healthcare innovation in the developing world means more than investing in technology. [Online]
Available at: https://news.trust.org/item/20170821144058-29rg6/
[Accessed 2019].

Chung, S.H., Sah, B., Lee, J., 2020. Optimization for drone and drone-truck combined operations: A review of the state of the art and future directions. Computers & Operations Research 123, 105004. https://doi.org/10.1016/j.cor.2020.105004

Claesson, A. et al., 2017. Time to Delivery of an Automated External Defibrillator Using a Drone for Simulated Out-of-Hospital Cardiac Arrests vs Emergency Medical Services. JAMA, 317(22), pp. 2332-2334.

Denby, S., 2019. The Super-Fast Logistics of Delivering Blood By Drone. [Online]
Available at: https://www.youtube.com/watch?v=bnoUBfLxZz0
[Accessed 2019].

Daganzo, C.F., 1984. The distance traveled to visit N points with a maximum of C stops per vehicle: An analytic model and an application. Transportation science, 18(4), pp.331-350.

Daganzo, C., Gayah, V. and Gonzales, E., 2012. The Potential of Parsimonious Models for Understanding Large Scale Transportation Systems and Answering Big Picture Questions. EURO Journal on Transportation and Logistics, Volume 1(1-2), pp.47–65.

Davis, B. A., and Figliozzi, M. A., 2013. A Methodology to Evaluate the Competitiveness of Electric Delivery Trucks. Transportation Research Part E: Logistics and Transportation Review, 49(1), 8-23.

Dennis, S. (2018). 'The ticking time bomb of e-commerce returns,' Forbes,14 Feb [online]. Available at: https://www.forbes.com/sites/stevendennis/2018/02/14/the-ticking-time-bomb-of-e-commerce-returns/#5ebaaa7c4c7f (Accessed 20 July 2019).

eMarketer. (2018a). Online shopping and buying-related activities performed by internet users in the United States as of March 2018, by age. Statista. Statista Inc. Available at: https://www.statista.com/statistics/868862/online-shopping-buying-related-activities-internet-users/ (Accessed: 5 June 2019).

eMarketer. (2018b). Primary reason that internet users in the United States make digital purchases as of March 2018. Statista. Statista Inc. Available at: https://www.statista.com /statistics/826773/primary-reasons-internet-users-make-digital-purchases/ (Accessed: 15 June 2019).

FAA, (2016), Federal Aviation Administration. Summary of Small Unmanned Aircraft Rule (Part 107). 21 June, 2016. https://www.faa.gov/uas/media/Part_107_Summary.pdf

Feng, W., Figliozzi, M., An Economic and Technological Analysis of the Key Factors Affecting the Competitiveness of Electric Commercial Vehicles, 2012 Transportation Research Part C, Volume 26, pp 135-145, 2013

Figliozzi, M., 2008. Planning Approximations to the Average Length of Vehicle Routing Problems with Varying Customer Demands and Routing Constraints. Transportation Research Record (2089), 1-8.

Figliozzi, M.A., 2011. The impacts of congestion on time-definitive urban freight distribution networks CO2 emission levels: Results from a case study in Portland, Oregon. Transportation Research Part C: Emerging Technologies, 19(5), pp.766-778.

Figliozzi, M., 2017. Lifecycle modeling and assessment of unmanned aerial vehicles (Drones) CO2e emissions, Transportation Research Part D: 2017, 57, 251-261.

Forbes, 2019, Amazon's New Delivery Drone Will Start Shipping Packages 'In A Matter Of Months', Available at: https://www.forbes.com/sites/jilliandonfro/2019/06/05/amazon-new-delivery-drone-remars-warehouse-robots-alexa-prediction/#7ac8ad4b145f (Accessed 25 August, 2019).

Frischmann, T., Hinz, O. and Skiera, B. (2014). Retailers' use of shipping cost strategies: Free shipping or partitioned prices? International Journal of Electronic Commerce, 16(3), pp. 65-88.

Gevaers, R., Van de Voorde, E. and Vanelslander, T. (2014). Cost modelling and simulation of last-mile characteristics in an innovatice B2C supply chain environment with implications on urban areas and cities. Procedia – Social and Behavioral Sciences, 125, pp. 398-411. doi: 10.1016/j.sbspro.2014.01.1483

Glick, T.B., Figliozzi, M., Unnikrishnan, A., 2021. A Case Study of Drone Delivery Reliability for Time-Sensitive Medical Supplies with Stochastic Demand and Meteorological Conditions. Transportation Research Record.

Glover, M. & Colton, T., 2019. Workhorse Partners with USOG to Launch Pilot Programs for Drone Delivery of Medical Supplies. [Online]
Available at: https://www.biospace.com/article/releases/workhorse-partners-with-usog-to-launch-pilot-programs-for-drone-delivery-of-medical-supplies/
[Accessed 2019].

Halldórsson, Á., Kovács, G., Edwards, J.B., McKinnon, A.C. and Cullinane, S.L., 2010. Comparative analysis of the carbon footprints of conventional and online retailing. International Journal of Physical Distribution & Logistics Management.

Jennings, D., Figliozzi, M., 2019. Study of sidewalk autonomous delivery robots and their potential impacts on freight efficiency and travel. Transportation Research Record 2673, 317–326.

Jennings, D., Figliozzi, M.A., 2020. A Study of Road Autonomous Delivery Robots and Their Potential Impacts on Freight Efficiency and Travel. Transportation Research Record.

Keeling, K. and Figliozzi, M. A. (2019). Impact of New Grocery E-Delivery Services on Travel Patterns, Access, and Equity [presentation]. METRANS 2019 International Urban Freight Conference, 18 October, Long Beach, CA.

Kirschstein, T., 2020. Comparison of energy demands of drone-based and ground-based parcel delivery services. Transportation Research Part D: Transport and Environment, 78, p.102209.

Kim, S.J., Lim, G.J., Cho, J., 2018. Drone flight scheduling under uncertainty on battery duration and air temperature. Computers & Industrial Engineering 117, 291–302. https://doi.org/10.1016/j.cie.2018.02.005

Kumar, N. and Ruan, R. (2006). On manufacturers complementing the traditional retail channel with a direct online channel. Quantitative Marketing and Economics, 4, pp. 289-323. doi: 10.1007/s11129-005-9003-8

Lee, D.Y., Thomas, V.M. and Brown, M.A., 2013. Electric Urban Delivery Trucks: Energy Use, Greenhouse Gas Emissions, and Cost-Effectiveness. Environmental science & technology, 47(14), pp. 8022-8030.

Lee, J., 2017. Optimization of a modular drone delivery system, in: 2017 Annual IEEE International Systems Conference (SysCon). Presented at the 2017 Annual IEEE International Systems Conference (SysCon), IEEE, Montreal, QC, Canada, pp. 1–8. https://doi.org/10.1109/SYSCON.2017.7934790

Li, Z., Brissette, F. & Chen, J., 2013. Finding the most appropriate precipitation probability distribution for stochastic weather generation and hydrological modelling in Nordic watersheds. Hydrological Processes, Volume 27, pp. 3718-3729.

Macrina, G., Di Puglia Pugliese, L., Guerriero, F., Laporte, G., 2020. Drone-aided routing: A literature review. Transportation Research Part C: Emerging Technologies 120, 102762. https://doi.org/10.1016/j.trc.2020.102762

Mell, H. K. et al., 2017. Emergency Medical Services Response Times in Rural, Suburban, and Urban Areas. JAMA surgery, 152(10), pp. 983-984.

microdrones, 2019. The Heavy-Lifting Drone md4-3000. [Online]
Available at: https://www.microdrones.com/en/drones/md4-3000/
[Accessed 2019].

Ministry of Infrastructure, 2012. Public Transport Policy and Strategy for Rwanda, Kigali: s.n.

Murray, C.C., Chu, A.G., 2015. The flying sidekick traveling salesman problem: Optimization of drone-assisted parcel delivery. Transportation Research Part C: Emerging Technologies 54, 86–109. https://doi.org/10.1016/j.trc.2015.03.005

NOAA, 2019. Climate Data Online. [Online]
Available at: https://www.ncdc.noaa.gov/cdo-web/
[Accessed 2017].

Nordenskjöld, A. M. et al., 2019. Circadian onset and prognosis of myocardial infarction with non-obstructive coronary arteries (MINOCA). PLOS ONE, Volume 4, p. 14.

Otto, A., Agatz, N., Campbell, J., Golden, B., Pesch, E., 2018. Optimization approaches for civil applications of unmanned aerial vehicles (UAVs) or aerial drones: A survey. NETWORKS 72, 411–458. https://doi.org/10.1002/net.21818

Pulver, A. & Wei, R., 2018. Optimizing the Spatial Location of Medical Drones. Applied Geography, Volume 90, pp. 9-16.

PYMNTS. (2018). Amazon retail e-commerce sales in the United States from 2014 to 2018, by product category (in million U.S. dollars). Statista. Statista Inc. Available at: https://www.statista.com/statistics/979781/amazon-retail-e-retail-sales-by-product-category-usa/ (Accessed: June 30, 2020.

Qin, Z., Li, W. & Xionga, X., 2011. Estimating wind speed probability distribution using kernel density method. Electric Power Systems Research, 81(12), pp. 2139-2146.

Rabta, B., Wankmüller, C., Reiner, G., 2018. A drone fleet model for last-mile distribution in disaster relief operations. International Journal of Disaster Risk Reduction 28, 107–112. https://doi.org/10.1016/j.ijdrr.2018.02.020

Rickert, J., 2016. Simulating from the Bivariate Normal Distribution in R. [Online] Available at: https://blog.revolutionanalytics.com/2016/08/simulating-form-the-bivariate-normal-distribution-in-r-1.html
[Accessed 2019].

Samadani, E., 2015. Modeling of Lithium-ion Battery Performance and Thermal Behavior in Electrified Vehicles, Waterloo, Ontario, Canada: University of Waterloo.

Scalea, J. R. et al., 2018. An Initial Investigation of Unmanned Aircraft Systems (UAS) and Real-Time Organ Status measurement for Transporting Human Organs. IEEE Journal of Translational Engineering in Health and Medicine, Volume 6, pp. 1-7.

Shao, X. F. (2017). Free or calculated shipping: Impact of delivery cost on supply chains moving to online retailing. International Journal of Production Economics, 191, pp.267-277.

Stöcker, C., Bennett, R., Nex, F., Gerke, M., Zevenbergen, J., 2017. Review of the Current State of UAV Regulations. Remote Sensing 9, 459. https://doi.org/10.3390/rs9050459

Simpson, J., Mishra, S., Talebian, A. and Golias, M., 2019. An Estimation of the Future Adoption Rate of Autonomous Trucks by Freight Organizations. Forthcoming Research in Transportation Economics.

Sorensen, H., Bogomolova, S., Anderson, K., Trinh, G., Sharp, A., Kennedy, R., Page, B. and Wright, M., 2017. Fundamental patterns of in-store shopper behavior. Journal of Retailing and Consumer Services, 37, pp.182-194.

Statista Survey. (2017a). How far do shipping costs influence your purchase decision when shopping online? Statista. Statista Inc. Available at: https://www.statista.com/statistics/705994/ influence-of-shipping-costs-on-purchase-decision-in-the-us/ (Accessed 28 June 2020).

Statista Survey. (2017b). Projected share of online holiday spending according to consumers in the United States as of October 2017, by urbanity. Statista. Statista Inc. Available at: https://www.statista.com /statistics/634065/projected-share-of-us-online-holiday-spending-urbanity/ (Accessed: 28 June 2020).

Statista Survey. (2017c). What percentage of items you order online do you return? Statista. Statista Inc. Available at: https://www.statista.com/statistics/706572/percentage-of-returning-online-orders-in-the-us-by-item/ (Accessed: June 29, 2020).

Statista Survey. (2018). Retail e-commerce sales in BRIC countries in from 2016 to 2023 (in million U.S. dollars). Statista Inc. Available at:

https://www.statista.com/statistics/255268/bric-b2c-e-commerce-sales/ (Accessed: 25 June 2020).

Suel, E., Le Vine, S. and Polak, J., 2015. Empirical application of expenditure diary instrument to quantify relationships between in-store and online grocery shopping: case study of Greater London. Transportation Research Record, 2496(1), pp.45-54.

Sutherland, B. (2019). ‘Amazon Threat to FedEx Is No Longer Fantastical’, Bloomberg via Washington Post, 24 June [online]. Available at: https://www.washingtonpost.com/business/amazon-threat-to-fedex-is-no-longer-fantastical/2019/06/24 (Accessed: 20 July 2019).

Talebian, A. and Mishra, S., 2018. Predicting the adoption of connected autonomous vehicles: A new approach based on the theory of diffusion of innovations. Transportation Research Part C: Emerging Technologies, Volume 95, pp. 363–380.

Thibbotuwawa, A., Bocewicz, G., Radzki, G., Nielsen, P., Banaszak, Z., 2020. UAV Mission Planning Resistant to Weather Uncertainty. Sensors 20, 515. https://doi.org/10.3390/s20020515

Tipagornwong, C. and Figliozzi, M. A. (2014). Analysis of the Competitiveness of Freight Tricycle Delivery Services in Urban Areas. Transportation Research Record, 2410

Torabbeigi, M., Lim, G.J., Kim, S.J., 2020. Drone Delivery Scheduling Optimization Considering Payload-induced Battery Consumption Rates. J Intell Robot Syst 97, 471–487. https://doi.org/10.1007/s10846-019-01034-w

Ungerleider, N. (2016). ‘Free Shipping is a Lie’, Fast Company, 1 Nov [online]. Available at: https://www.fastcompany.com/3061686/free-shipping-is-a-lie (Accessed on 21 July 2019).

U.S. Forest Service, 2019. If You Fly, We Can't. [Online]
Available at: https://www.fs.usda.gov/managing-land/fire/uas/if-you-fly
[Accessed 2020]

11.0 APPENDIX

The time constraint is represented by the following equation:

$$\tau = \left(\frac{2d}{v} + \frac{k_l}{mv_l}\sqrt{an}\right) + \frac{t\,n}{m}$$

Rearranging terms

$$\tau - \frac{2d}{v} - \frac{tn}{m} = \frac{k_l\sqrt{an}}{mv_l}$$

Squaring both sides

$$\left(\frac{k_l\sqrt{an}}{mv_l}\right)^2 = \left(\tau - \frac{2d}{v} - \frac{t}{m}n\right)^2$$

Introducing the following notation to simplify notation

$$y_a = \left(\tau - \frac{2d}{v}\right)$$

$$y_{cm} = \left(\frac{t}{m}\right)$$

$$y_{lm} = \left(\frac{k_l\sqrt{a}}{mv_l}\right)$$

Replacing

$$n\,{y_{lm}}^2 = (y_a - y_{cm}n)^2$$

$${y_{lm}}^2\,n = {y_a}^2 - 2\,y_a y_{cm} n + {y_{cm}}^2\,n^2$$

$$({y_{cm}}^2)\,n^2 - (2\,y_a y_{cm} + {y_{lm}}^2)n + ({y_a}^2) = 0$$

$$n^2 - \frac{(2\, y_a y_{cm} + y_{lm}{}^2)}{(y_{cm}{}^2)} n + \frac{(y_a{}^2)}{(y_{cm}{}^2)} = 0$$

Solving the second order equation

$$n = \frac{(2\, y_a y_{cm} + y_{lm}{}^2)}{2\,(y_{cm}{}^2)} \pm \left(\frac{1}{4} \left(\frac{2\, y_a y_{cm} + y_{lm}{}^2}{y_{cm}{}^2} \right)^2 - \left(\frac{y_a}{y_{cm}} \right)^2 \right)^{1/2}$$

$$n = \frac{(2\, y_a y_{cm} + y_{lm}{}^2)}{2\,(y_{cm}{}^2)} \pm \left(\frac{1}{4} \left(\frac{4\, y_a y_{cm} y_{lm}{}^2 + y_{lm}{}^4}{y_{cm}{}^4} \right) \right)^{1/2}$$

Only the negative root is feasible

$$n = \frac{1}{2\, y_{cm}{}^2} \left[(2\, y_a y_{cm} + y_{lm}{}^2) - (4\, y_a y_{cm} y_{lm}{}^2 + y_{lm}{}^4)^{1/2} \right]$$

Replacing the previously defined y terms

$$n = \frac{1}{2\left(\frac{t}{m}\right)^2} \left[\left(2\left(\tau - \frac{2d}{v}\right)\left(\frac{t}{m}\right) + \left(\frac{k_l\sqrt{a}}{m v_l}\right)^2 \right) - \left(4\left(\tau - \frac{2d}{v}\right)\left(\frac{t}{m}\right)\left(\frac{k_l\sqrt{a}}{m v_l}\right)^2 + \left(\frac{k_l\sqrt{a}}{m v_l}\right)^4 \right)^{1/2} \right]$$

$$n = \frac{m^2}{2\, t^2} \left[\left(2\left(\tau - \frac{2d}{v}\right)\left(\frac{t}{m}\right) + \left(\frac{k_l\sqrt{a}}{m v_l}\right)^2 \right) - \left(4\left(\tau - \frac{2d}{v}\right)\left(\frac{t}{m}\right)\left(\frac{k_l\sqrt{a}}{m v_l}\right)^2 + \left(\frac{k_l\sqrt{a}}{m v_l}\right)^4 \right)^{1/2} \right]$$

Or

$$n = \frac{\left(2\left(\tau - \frac{2d}{v}\right)\left(\frac{t}{m}\right) + \left(\frac{k_l\sqrt{a}}{mv_l}\right)^2\right)}{2\left(\frac{t}{m}\right)^2} - \left(\frac{4\left(\tau - \frac{2d}{v}\right)\left(\frac{t}{m}\right)\left(\frac{k_l\sqrt{a}}{mv_l}\right)^2 + \left(\frac{k_l\sqrt{a}}{mv_l}\right)^4}{4\left(\frac{t}{m}\right)^4}\right)^{1/2}$$